8-2012

Determining the Motion and Location of the Frenchman Mountain Fault, Las Vegas, Nevada: A Paired Basin Analysis and Structural Analysis

Laura Margaret Eaton
University of Nevada, Las Vegas

DETERMINING THE SIGNIFICANCE AND SENSE OF OFFSET OF THE FRENCHMAN MOUNTAIN FAULT LAS VEGAS, NEVADA: A PAIRED BASIN ANALYSIS AND STRUCTURAL ANALYSIS

by

Laura Margaret Eaton

Bachelor of Science
University of St. Thomas
2007

A thesis submitted in partial fulfillment
of the requirements for the

Master of Science in Geoscience

Department of Geoscience
College of Science
Graduate College

University of Nevada, Las Vegas
August 2012

THE GRADUATE COLLEGE

We recommend the thesis prepared under our supervision by

Laura Margaret Eaton

entitled

Determining the Significance and Sense of Offset of the Frenchman Mountain Fault Las Vegas, Nevada: A Paired Basin Analysis and Structural Analysis

be accepted in partial fulfillment of the requirements for the degree of

Master of Science in Geoscience
Department of Geoscience

Andrew Hanson, Committee Chair

Gene Smith, Committee Member

Wanda Taylor, Committee Member

Susan Meacham, Graduate College Representative

Thomas Piechota, Ph. D., Interim Vice President for Research and Graduate Studies and Dean of the Graduate College

August 2012

ABSTRACT

Determining the Motion and Location of the Frenchman Mountain Fault, Las Vegas, Nevada: A Paired Basin Analysis and Structural Analysis

by

Laura Margaret Eaton

Dr. Andrew Hanson, Examination Committee Chair
Associate Professor of Geology
University of Nevada, Las Vegas

Understanding the evolution of large-scale fault systems remains a challenge to geologists and is of critical importance in understanding the dynamics of larger plate tectonic interactions. I mapped the southwestern Frenchman Mountain Fault (FMF), conducted a basin analysis of units in the footwall of the fault, and measured kinematic indicators along the fault zone in order to constrain fault offset, magnitude, and timing in an attempt to further our understanding of these systems.

My findings include: 1) the presence of vertical and sub-vertical slickenlines on southwest dipping fault surfaces indicative of normal sense offset; 2) relatively little lateral variation in stratigraphy within the adjacent basin indicating basin-fill being shed directly across the fault, supported by paleocurrent data; and 3) no kinematic evidence indicative of strike-slip motion. I conclude that normal sense displacement on the fault ceased prior to deposition of the Red Sandstone. In addition, I hypothesize that the southwestern FMF is not the Frenchman Mountain block-bounding fault; instead it is buried beneath younger sediments farther to the southwest.

ACKNOWLEDGEMENTS

The undertaking and ultimate completion of this thesis is the amalgamation of work from many individuals, all of whom I cannot possibly thank properly. First and foremost, I must thank my advisor Dr. Andrew Hanson for sparking my interest in this project, and for his contagious zeal and passion for geology. The hours spent in the field and office discussing and working on this thesis with Dr. Hanson were invaluable to the success of this work. I would also like to give a special thanks to my committee members, Dr. Wanda Taylor, Dr. Eugene Smith, and Dr. Susan Meacham for their helpful discussions, critiques and insights. Additional helpful conversations with Dr. Scott Nowicki, Dr. Adam Simon, Dr. Rodney Metcalf, Dr. Ganqing Jiang, Dr. Brenda Buck, Ernie Anderson, Jim O'Donnell, Nicholle Booker, and Rebecca Huntoon were integral to the success of this project. This work was made possible because of the efforts of all of the previous researchers, geologists, and desert rats that have roamed the southwestern United States before me and paved the way for us.

The foundation for this thesis was laid in the department of geology at the University of St. Thomas. I owe a debt of gratitude to Dr. Lisa Lamb and Dr. Tom Hickson for instilling in me a passion for geology by showing me what it means to be a true geologist; for this I am forever grateful. I also had an immense amount of support and help from my fellow geologists at UNLV in the field, classroom, and everywhere in between. Special thanks goes to: Swapan, Corinne, Mandy, James, Bobby, Jason, Steven, Nate, Brian, Vicki, Jeevan, Tom, Allison, Lindsay, Josh, Aubrey, Meg, Aaron, Carl, Nick, Kelly, Denise, LaOde, Adam, Yuki, and Michael. Thank you.

This thesis was made possible from generous funding from the department of Geoscience at UNLV and the Nevada Petroleum Society. Special thanks to Cathy Willy with assistance in permitting with the Bureau of Land Management.

I would like to dedicate this thesis to my friends and family who have been with me on this journey and have supported me. Most importantly mom, dad, Todd, and Sarah; this thesis would not have been possible without you.

TABLE OF CONTENTS

LIST OF FIGURES

LIST OF PLATES

CHAPTER 1

INTRODUCTION

Understanding the behavior and evolution of large-scale fault systems within extensional terrains is a critical component in understanding the dynamic geologic processes of plate tectonics. The Basin and Range province of western North America is a world-class example of an extensional system but is still not completely understood because it is highly variable and geologically complex. The province is relatively young and geographically extensive. Numerous studies focus on the geology of the Basin and Range, and many state that much still remains to be understood and recognize the need for further investigation. The Lake Mead region is of particular importance because of its location within the Central Basin and Range (CBR) (Fig. 1): the transition between the northern Basin and Range and the southern Basin and Range. The CBR is the youngest, most complex, and arguably the least understood sub-province within the Basin and Range. For this reason, the Lake Mead region is an ideal laboratory for understanding how fault systems evolve. It is also ideal in that the pre-extensional geology of the Lake Mead region is relatively straight forward, and excellent exposures allow geologic reconstructions more easily than in other areas of the region (Wernicke et al., 1988; Duebendorfer and Simpson, 1994). Therefore, studying structures and basins within the Lake Mead region is integral to understanding how the region itself has evolved over time, allowing for extrapolation about the evolution of the CBR and greater Basin and Range.

Various authors have proposed differing hypotheses on the extensional direction, magnitude, and timing of Miocene extension in the Lake Mead region. Most notably

Anderson (1971), Longwell (1974), Bohannon (1979), Angelier and others (1985), Wernicke and others (1988), and Fryxell and Duebendorfer (1990) have all interpreted the extensional genesis of the Miocene Lake Mead region. For this reason, it is especially important to find structural blocks that act as markers to constrain offset and understand the extensional development of the region. The Frenchman Mountain Block (FMB) (Fig. 2) has been used by numerous researchers as such a marker to estimate the magnitude and orientation of extension (Longwell, 1974; Bohannon, 1979, 1984; Wernicke et al., 1988; Fryxell and Duebendorfer, 1990, 2005; Rowland et al., 1990).

Previous researchers concluded that the FMB is bound on its west and southwest sides by the Frenchman Mountain Fault (FMF). While much attention has been paid to understanding the translation of the FMB, a detailed study of the FMF has not been done and could potentially change how researchers interpret the most recent movement of the FMB as well as extensional geologic reconstructions of the Lake Mead region. Previous researchers have cited and mapped the FMF as having contradictory senses of offset: some researchers classify the fault solely as a normal fault (Langenheim et al., 2001) and others maintain that the fault experienced both strike-slip and normal displacement (Castor et al., 2000). Located on the eastern edge of the Las Vegas Valley, the FMF consists of two main portions: a roughly N-S fault system along the western edge of Frenchman Mountain and a NW-SE trending fault system along the western edge of the FMB. This study dealt with the later of these two faults systems near the intersection of two major strike-slip systems in southeastern Nevada, the Las Vegas Valley shear zone and the Lake Mead fault system, and lies in a zone of extremely complex geology (Fig. 2). For clarity sake, I herein refer to the portion of the FMF within the map area as the

southwestern FMF (SW FMF) in order to distinguish it from the portion of the FMF that is exposed at the western base of Frenchman Mountain, which I refer to as the western FMF (WFMF). Castor et al. (2000) have completed the most detailed work on the fault to date, but acknowledge that no systematic studies have dealt specifically with the fault and that further research needs to be completed.

This study uses the approach of integrating basin and structural analysis techniques in order to determine fault evolution. I completed detailed geologic mapping along the previously mapped SW FMF (Bell and Smith, 1980; Castor et al., 2000) and paired it with a stratigraphic basin analysis study of the basin that lies to the southwest of the SW FMF. If offset on the SW FMF impacted how the basin adjacent to it filled, documentation of provenance and basin evolution of the basin fill, as well as kinematic analysis and mapping, allows for extrapolation of fault offset sense, magnitude, and timing.

My goal was to test two competing hypotheses: 1) the SW FMF is a strike-slip fault, and, 2) the SW FMF is the result of oblique normal faulting. Any determination of the sense of offset and its significance clarifies the role of the FMF within the Lake Mead region, thus allowing for refined interpretations about the CBR and our understanding of how large-scale extensional fault systems evolve through time.

CHAPTER 2

GEOLOGIC HISTORY

Western North America

Understanding the geologic development of western North America is necessary for appreciating the complexity of the Lake Mead region for understanding the evolution of the SW FMF. Precambrian western North America consisted of various major sedimentary packages that overlay accreted crystalline basement. Varying structural grains of the basement units are a result of deformation prior to the Late Proterozoic, and the relationships between the basement and overlying sedimentary rocks record several deformation events within the continent (Burchfiel et al., 1992). In the Late Paleozoic a rift developed along the entire western margin of North America, resulting in the inception of a passive margin and the deposition of a westward thickening succession of sedimentary rocks (Burchfiel et al., 1992). From the Late Devonian to the Late Jurassic western North America experienced several successive deformational events resulting from the accretion and thrusting of numerous terrains in the Antler, Sonoma, and Nevada orogenies (Schweickert et al., 1984; Trexler et al., 1991; Burchfiel et al., 1992). The Permian to Jurassic marks the beginning of the development of both the Central Nevada fold and thrust belt, and the Sevier thrust belt, both composed of a series of dominantly east-vergent folds and thrust faults (Taylor and Switzer, 2001). In addition to these two major features, the Sevier orogeny is marked by westward underthrusting, the development of an elevated hinterland, and a foreland basin (Burchfiel et al., 1992; Druschke et al., 2008). Initiating after, and partially overlapping the Sevier, the Laramide orogeny occurred and involved flat slab subduction, perhaps due to the buoyancy of the

down going slab, making the subducting slab come in direct contact with the overlying continental crust (Humphreys et al., 2003). This long history of orogenic and deformational events left the lithosphere of western North America dehydrated, weakened, and thickened; particularly susceptible to extension.

During the late Mesozoic and early Cenozoic the western margin of North America was a convergent plate boundary between the subducting Farallon plate and the overriding North American plate (Sonder and Jones, 1999). At about 52 Ma the Farallon plate broke into the Vancouver (future Juan de Fuca) and Farallon plates, with the Farallon plate to the east and the Vancouver to the west. The Vancouver plate converged with the North American plate at an oblique angle, and some researchers have hypothesized that the associated shearing could have caused extension before 30 Ma (Sonder and Jones, 1999). Around 27-16 Ma the Farallon plate further fragmented and experienced a combination of subduction and strike-slip motion, and the plate margin became a transform fault bounded by the Mendocino triple junction on the north, which moved north with time (Sonder and Jones, 1999). Accordingly, models that suggest that extension before 30 Ma was driven by oblique convergence further hypothesize that post 30 Ma right-lateral motion of the transform boundary resulted in shearing that caused extension (Sonder and Jones, 1999).

Basin and Range Extension: Central Basin and Range

The pre-Eocene to recent extension of western North America caused the lithosphere to have extreme differences in composition, rheology, strain, and structural grains (Humphreys et al., 2003). Beginning sometime in the Eocene to Oligocene the

Basin and Range province developed and is characterized by sweeping magmatism, complex tectonic patterns, and extreme extension (Sonder and Jones, 1999) (Fig. 1). The Basin and Range region is divided into three provinces, the Northern Basin and Range (NBR), the Central Basin and Range (CBR), and the Southern Basin and Range (SBR) as shown in Figure 1. The FMF is located within the CBR province and Wernicke et al. (1988) estimated that from the Miocene to present day it has experienced approximately 250 km of extension, a factor of 3-4, the most dramatic extension in all three provinces. This province is also unique in that its onset of extension significantly post-dates the onset of extension and magmatism of both the NBR and the SBR (Fig. 1). Initiation of extension and magmatic activity in the CBR is late Oligocene-Miocene in age, while the NBR and SBR experienced extension in the Eocene-Oligocene (Fig. 1) (Beard, 1996; Sonder and Jones, 1999). New evidence from Druschke et al. (2009) suggests that extension occurred in the NBR as early as the Late Cretaceous based on the presence of major syndepositional normal faults, megabreccia deposition, and fanning of dips within the Sheep Pass Formation. The CBR has the greatest local relief; displays large north-south gradients in topography, heat flow and gravity; and is tectonically and volcanically active (Sonder and Jones, 1999).

The Lake Mead region at the latitude of Las Vegas within the CBR is an ideal place to study extensional geometries because its pre-extension geology is relatively straightforward as Cordilleran passive margin sequence rocks are exposed across the entire province (Wernicke et al., 1988). It is also of unique importance because its location represents the transition from the Northern Basin and Range (NBR) to the Southern Basin and Range (SBR) and is the narrowest section of the Basin and Range;

both characteristics make this area the most complicated and least understood portion of the province. Wernicke et al. (1988) focused on the relatively low-lying geology at the latitude of Las Vegas, from the Sierra Nevada to the Colorado Plateau as a type example of the structural patterns observed within the CBR. The geology is divided into two major extensional domains; the Las Vegas Valley and Death Valley, which are separated by a relatively unextended block. These domains are deformed by generally east-vergent Mesozoic thrust faults that are ideal for geologic reconstructions and both fault systems are reactivated faults within the older thrust systems (Wernicke et al., 1988). Examination of structural relationships in the field have allowed for a better understanding of the timing of Basin and Range extension, revealing that extension in the CBR slowed with time perhaps recording a significant tectonic event or response of the lithosphere. Fault geometries evolved from early low-angle normal faults to the development of widespread high-angle normal faults, which has been hypothesized to have aided in slowing extension (Wernicke et al., 1988). The movement of both systems has resulted in approximately 250 km of extension between the Las Vegas and Death Valley fault systems and constrain the majority of extension to have occurred during 15 Ma to present time, while approximately 100 km of extension occurred before 15 Ma (Wernicke et al., 1988). Wernicke et al. (1988) documented movement of the Sierra Nevada away from the Colorado Plateau at an approximate rate of 20-30 mm/year between 15-10 Ma. From 10 Ma to present time extension slowed to its current rate of 10 mm/year (Wernicke et al., 1988).

Wernicke et al. (1982) suggest that widespread imbricate normal fault blocks and subadjacent large low-angle normal faults can account for a large amount of extension,

reflected in “chaos structures” and field relationships documented in the Basin and Range. Basin and Range large scale extension was accommodated by large displacement on low-angle normal faults without rotation, as well as rotation of faults and fault blocks through listric and planar geometries (Wernicke et al., 1982). Vector analysis and field observations reveal strike-slip faulting to be an important component in the extending system and absorbed approximately 40-50 km of north-south shortening in the region (Wernicke et al., 1988). Observation of this strike-slip motion might reflect the constriction of the CBR, as well as its transitional position relative to the NBR and SBR; the entire length of the FMF is one such structure that has been interpreted as a strike-slip fault (Wernicke et al., 1988).

Lake Mead Regional Geology

The FMF is located near the three most significant structural features in the Lake Mead region; the northwest striking Las Vegas Valley shear zone (LVVSZ), the northeast striking Lake Mead fault system (LMFS), and the Saddle Island detachment fault (SIDF), a west-dipping low-angle detachment fault (Fig. 2) (Fryxell and Duebendorfer, 2005). All three fault systems initiated during Cenozoic extension and their intersection has created a zone of extremely complex geology, specifically the LVVSZ and the LMFS (Campagna and Aydin, 1994). The LVVSZ is composed of a series of right-lateral faults that have accommodated approximately 48 ± 7 km of displacement, the majority of this occurring after 13 Ma (Duebendorfer and Simpson, 1994). The exact location, geometry, and sense of offset of this fault system is contentious due in large part to the poor exposure attributed to burial beneath alluvial deposits that fill the Las Vegas Valley

(Langenheim et al., 2001). Longwell (1974) approximated that the LVVSZ strikes N 60 W, while Campagna and Aydin (1994) say it is closer to a strike of N 45 W. The LMFS is a major fault system composed of a series of faults with apparent left-lateral displacement. Timing of movement on the fault system has been loosely constrained to 17 and 10 Ma, and has accounted for approximately 20 to 65 km of displacement (Duebendorfer and Simpson, 1994).

Within the Lake Mead region there are three main structural blocks that are distinct based upon their structural and depositional (stratigraphic) characteristics: the Frenchman Mountain block (FMB), the Muddy Mountains block (MMB), and the Boulder Basin block (BBB) (Fig. 2). The stratigraphic variations and correlation between the three blocks have been described in detail by previous researchers (i.e., Duebendorfer and Simpson, 1994), thus will not be discussed in full detail here. I focused on the FMB in light of its relevance to the history of the SW FMF, and its detailed stratigraphy is discussed in a later section. The FMB is an allochthonous homocline that dips to the east at 45°-55°, and has been hypothesized to have been translated 60-70 km to the west, originating in the Gold Butte area (Fig. 2) (Rowland et al., 1990; Fryxell and Duebendorfer, 2005). This hypothesis is based on correlation of basal Cenozoic sections, and debris-flow and megabreccia deposits within the Thumb Member of the Horse Spring Formation that could have only originated adjacent to the Gold Butte block (Rowland et al., 1990). That study further concluded that orientations of eolian cross-bedding within the Aztec Sandstone in the FMB are identical to those found in the Gold Butte block, suggesting that the FMB did not experience significant rotation during its translation (Rowland et al., 1990). While the geographic origin of the FMB is nearing acceptance by

the main workers in the area, identifying the structure or structures that accomplished this translation has proven difficult. Researchers have proposed various methods of translation of the FMB including via both the LVVSZ (Longwell, 1971, 1974), and the LMFS (Bohannon, 1979, 1984), but subsequent studies have disagreed with both of these hypotheses as well as others (Fryxell and Duebendorfer, 2005).

Larger questions concerning the sense of offset and location of the LMFS and the LVVSZ still remain and serve as examples of large-scale fault systems in the area that are not fully understood. Previous mapping shows the WFMF offsets Quaternary units along the west side of the FMB which indicates that the region has remained tectonically active post translation from its original position 60-70 km to the east from the Gold Butte block (Rowland et al., 1990).

Weber and Smith (1987) proposed that the River Mountains and the FMB were structurally adjacent to each other by 13 Ma because of dated lavas that interfinger with the Bitter Ridge Limestone Member of the Horse Spring Formation in the FMB. The FMF has been cited as having multiple strands (Castor et al., 2000) and has also been suggested to be related to both the Boulevard fault (BF) and Munitions fault (MF) zones (Fig. 3), perhaps having transferred some of its motion to these fault systems (Castor et al., 2000). These suggestions further underscore the importance of determining the sense of motion of this fault, as it will lead to interpretations about the MF and BF as well and in turn about the genesis of extension in the Lake Mead region.

CHAPTER 3

PREVIOUS WORK

As mentioned above, general consensus exists that the FMB originated approximately 60 km to the east near the Gold Butte block, based on detailed studies done by numerous authors, most notably and recently by Rowland et al. (1990). However, at least eight hypotheses existed previous to this one. These hypotheses have been described in detail and published by Fryxell and Duebendorfer (2005), which is the most recent to highlight the complexity and contentious nature of the debate of the previous location of the FMB. Inherently, if the origin of the FMB is still debated, the method of translation must also be unclear.

Previous Models

Numerous studies have been done in an attempt to determine the principle direction of Miocene extension within the Lake Mead region. Various authors support an extensional direction to the southwest (Anderson, 1971; Bohannon, 1979; Weber and Smith, 1987), some principally to the west (Wernicke et al., 1988; Rowland et al., 1990, Fryxell and Duebendorfer, 1990), west-northwest (Longwell, 1974), and others favor a dynamic extensional model that invokes changes in extensional directions through time (Angelier et al., 1985). Determining the direction of extension is integral in backing out what structures played significant roles in this extension and what sense of motion these structures experienced. Duebendorfer and Simpson (1994) state that the downfall of many of the previous studies has been that they focus only on one or two main structures to determine the extensional direction of the entire Lake Mead region. For this reason, it

is important to first understand the kinematic evolution of all of the main structures in the region and then synthesize the findings to extrapolate extensional direction on the larger scale. If it is possible to determine the most recent motion of the FMF by doing a detailed study, it is then possible to integrate its recent motion into previous models to see which are plausible. While many previous studies have dealt with the method of translation of the FMB, none have dealt specifically with the FMF itself.

Several seminal publications on the geology of the Lake Mead region have emphasized the need to further study strike-slip features and to view them as major structures that can have significant impact on the deformational development of a region, specifically in the Basin and Range province. Many researchers have interpreted and mapped the FMF as having exclusively strike-slip motion (Longwell, 1974; Bohannon, 1979, 1984; Ron et al., 1986; Anderson et al., 1994; Campagna and Aydin, 1994; Langenheim et al., 2001). The concept of the FMF being a strike-slip fault was originally proposed in Longwell's work (1974) on the LVVSZ. Later, Bohannon (1984) hypothesized that the FMB was translated westward along strands of the LMFS, based on the "piercing line" offset marker of the base of the unconformity. One of the more recent studies that interpreted the FMF as having solely strike-slip motion was done by Campagna and Aydin (1994), who further extrapolate that the FMF is part of a larger pull apart basin that formed the Las Vegas Valley. Basin geometries and the geometry of the LVVSZ based on geophysical surveys have resulted in their tentative mapping of the FMF as a right-lateral strike slip fault (Campagna and Aydin, 1994). Their study places the main strand of the LVVSZ on the northeast side of the FMB. Conversely, in the most recent publication dealing specifically with the FMF, done by Langenheim et al. (2001), a

major strand of the LVVSZ is mapped just west of where the FMF is located. Langenheim et al. (2001) mapped the northwestern FMB bounding fault as a normal fault, but interpret it as part of a larger pull-apart basin system.

Conversely, many other researchers have cited the importance of interaction between normal and strike-slip faults in the Lake Mead region. Both Anderson (1971) and Bohannon (1984) considered normal faults in the Lake Mead region to be genetically related to strike-slip faults. Additionally, Duebendorfer and Simpson (1994) suggested that the interaction between normal and strike-slip faults is the key to understanding how major fault systems evolve. Many researchers maintain that the offset of the FMF is a result of both strike-slip and normal fault motion (Guth, 1981; Wernicke et al., 1982; Weber and Smith, 1987; Rowland et al., 1990; Duebendorfer and Wallin, 1991; Duebendorfer et al., 1998; Fryxell and Duebendorfer, 2005). Most recently, Fryxell and Duebendorfer (2005) compiled all of the previous methods of translation and paleo position of the FMB and concluded that the FMB was once in the hanging wall of the Gold Butte block as part of the hanging wall of the Lakeside Mine fault. This is based on previously discussed correlations made by Rowland et al. (1990) as well as on thermochronology exhumation ages of the Gold Butte block (Fryxell and Duebendorfer, 2005).

My Approach

I completed a combination of fieldwork and laboratory analysis in order to gain an in-depth understanding of both the fault kinematics and basin composition, in order to test two hypotheses. By studying basin stratigraphy and provenance, and by

documenting fault kinematics, I tested the two stated hypotheses and helped constrain the timing of displacement.

The link between structure and stratigraphy is imperative, in that the relationships between them can be distinctly different depending on whether the SW FMF experienced normal or strike-slip motion. If the hypothesis that the SW FMF experienced solely normal-fault movement is supported, then the basin fill from west to east should be fairly compartmentalized stratigraphically, and slickenlines along the fault would be nearly vertically oriented (Fig. 4a). In this case, the sediment from the footwall source would be linked to discrete areas in the basin within the footwall. This would be constant through time resulting in the relative position of basin fill closely imitating the lithologies in its correlative sediment source area. The physical evidence of this relationship would be supported by relatively uniform stratigraphic sections which vary laterally but are relatively uniform vertically, and paleocurrent indicators within the basin fill that indicate a sediment source directly across the fault.

Conversely, if the SW FMF experienced solely strike-slip motion, stratigraphic and provenance relationships would be markedly different. These relationships will be much more complicated, and slickenlines would be horizontal or sub-horizontally oriented (Fig. 4b). In this case, the sediment from the footwall source would also shed into the basin, but because the basin would be moving relative to the source areas, the vertically stacked stratigraphy would reflect multiple, evolving sediment source areas through time. As opposed to the sediment sources being linked to the same discrete portion of the basin, it would be dynamic with time resulting in a more complex basin stratigraphy. Physical evidence supporting the strike-slip hypothesis would be found in

complex stratigraphic column relationships, as well as provenance sources being displaced across the fault plane.

Local Stratigraphy

The stratigraphy of this study area has been well defined by previous researchers, most notably: Bell and Smith (1980), Rowland et al. (1990), Duebendorfer and Simpson (1994), Castor et al. (2000), and Fryxell and Duebendorfer (2005). The stratigraphy encountered in the Mobil Oil Virgin 1A test well is representative of the general regional stratigraphy and is shown in Figure 5. The stratigraphy in the Lake Mead region is mainly Cenozoic sedimentary and volcanic units that are deposited in angular discordance on Triassic to Cretaceous rocks of the area, with the main exception of the Kingman Arch in which Cenozoic strata directly sits on Precambrian to Paleozoic basement (Duebendorfer and Simpson, 1994; Faulds et al., 2001). Stratigraphic units within my study area range from Permian to Quaternary in age. The Permian units are limited and typically occur within basin fill units as clasts, however some outcrops of the Kaibab and Toroweap Formations are present on the northeast side of the FMF. The Mesozoic units consist mainly of the various members of the Moenkopi Formation and outcrops are mainly limited to the footwall of the SW FMF in the map area, with the exception of one outcrop of the upper red member of the Moenkopi Formation which sits south of the SW FMF near the Sunrise Landfill. Neogene units are the most widespread units throughout the field area and are dominated by the Rainbow Gardens and Thumb Members of the Horse Spring Formation, but also include limited outcrops of the Bitter Ridge Limestone and the volcanic rocks of Rainbow Gardens. These units are exposed on both the southwest

and northeast sides of the FMF. A unit previously mapped as a member of the Muddy Creek Formation by Bell and Smith (1980) is reinterpreted here based of the findings of Rittase (2007) as being Red Sandstone (Tr), as defined by Bohannon (1984). The Red Sandstone mainly crops out on the southwest side of the FMF but in places overlaps the SW FMF. The gypsiferous member of the Muddy Creek Formation lies in angular unconformity over the underlying Cenozoic deposits and is only exposed within the hanging wall of the FMF.

CHAPTER 4

METHODS

Geologic Mapping

Central to this study is understanding geologic relationships proximal to the SW FMF; accordingly geologic mapping using standard geologic mapping techniques at a scale of 1:12,000 was done along the SW FMF and within the adjacent basin in order to refine work previously done in the area. The United States Geological Survey Henderson quadrangle mapped by Bell and Smith (1980), and Frenchman Mountain mapped by Castor et al. (2000), as well as the Beard et al. (2007) preliminary geologic map of the Lake Mead 30 x 60 quadrangle were used as reference maps during mapping in order to assure consistency in unit nomenclature as well as a field reference. The map area comprises 12.1 km^2 on the east side of the Las Vegas Valley (Fig. 2). The mapped area consists of an approximately 5.8 km long SW trending swath along the SW FMF, as well as the basin adjacent to the fault which extends outward to the southwest about 2.4 km. The field area was picked based on its location within the Lake Mead region, inclusion of the SW FMF, its relatively well-exposed units, and fairly well defined stratigraphy.

During geologic mapping, I used the nomenclature employed by Bell and Smith (1980) for the Henderson Quadrangle and by Castor et al. (2000) for the Frenchman Mountain Quadrangle. However these authors used different nomenclature for some units and therefore it was necessary to address these differences and determine what unit nomenclature would be used in this study. For the Thumb Member, I followed the unit nomenclature used by Castor et al. (2000). I initially followed the lead of Bell and Smith (1980) with regards to the main basin fill south of the fault and mapped these units as the

Muddy Creek Formation (Tmc) and Quaternary units. Based on reasoning explained later in this thesis, I concluded that what had been mapped as Tmc is actually Tr, so I mapped these units as Tr.

A Brunton compass was used to measure strike and dip of bedding as well as orientations of fault planes and kinematic indicators. Slickenlines were measured on fault planes and were recorded as trend and plunge data. Kinematic data were recorded throughout the field area, with particular attention being paid along the SW FMF, in order to identify any indicators that would signify fault motion. Following field collection of data, the techniques of Marrett and Allmendinger (1990) were used for graphical kinematic analysis using the Stereonet software developed by Allmendinger (2002). Standard kinematic analysis assumptions used are similar to those employed by Duebendorfer and Simpson (1994) as well as Marrett and Allmendinger (1990). Kinematic analysis was done both in the field and subsequently using the Allmendinger software to identify conjugate fault sets and patterns, as well as to determine the dominant strain patterns within the field area. A new geophysical technique using collection of passive low-frequency seismic data was done within the field area to try and determine fault location within the subsurface (Saenger et al., 2009). The results were inconclusive, but are included in Appendix VI.

Digital Data Entry

Digital data entry, mapping, and creation of three-dimensional images were completed using ArcGIS and Adobe Illustrator software suite. Following field data collection and mapping, geological positions and relationships observed were digitized

over base maps including digital orthographic quadrangles (DOQ), topographic maps from the United States Geological Survey, Quickbird imagery and various aerial photographs.

Stratigraphic Analysis

Understanding how the basin adjacent to the SW FMF has evolved is equally important as understanding the structural genesis because it potentially recorded response to fault movement. It was integral to understand stratigraphic relationships and how stratigraphy compared and contrasted with structural patterns to see if the two were somehow linked. Within the basin it was important to examine unit distribution, continuity, lateral variations in thickness or composition, as well as any structure that disrupted the expected depositional sequence. Standard provenance techniques were used in order to determine the source area as well as lateral variation throughout the basin. Conglomerate clast counts were conducted within the Tr in the field area along transects that are roughly perpendicular to the FMF, in order to determine whether deposits vary in composition or texture (clast size range) due to proximity to the fault. Transects are approximately 300 m in length, and along each transect three to five conglomerate clast counts with 100 clasts each were taken. Paleocurrent directions were also measured within the Tr along the same transects in order to tie the provenance and the transport directions in the unit. Paleocurrent data derived from imbricated clasts in the Tr were taken at two to three locations along each transect with ten measurements at each location. Two schematic cross sections were constructed to show structural and stratigraphic relationships within the field study area. Numerous ash samples were

collected within the field area in order to constrain timing of deposition or faulting, but none were deemed suitable for analysis; this will be discussed in further detail later on.

CHAPTER 5

DATA, RESULTS AND DISCUSSION

Geologic Mapping Data and Results

Detailed (~1:12,000) geologic mapping was done in the area where the SW FMF had been mapped by previous researchers (Bell and Smith, 1980; Castor et al., 2000), as well as in the basin adjacent to it and the results of mapping are shown in Plate 1. The SW FMF dips steeply to the SW in the field area so the footwall is to the northeast of the fault, while the hanging wall is on the southwest side of the fault. All of the field data including bedding orientations (Appendix III), and their location within the field area are shown in Plate 1. Although the main results of the mapping can be seen in Plate 1, it is necessary to further report major findings discovered while mapping.

Paleozoic, and most Mesozoic, units are found only in the footwall of the FMF in the map area (Plate 1). The only Mesozoic unit to crop out south of the FMF is the upper red mudstone member of the Moenkopi, which crops out in the hanging wall in the far western portion of the map adjacent to the Sunrise Landfill. Most Cenozoic units crop out in both the footwall and hanging wall of the FMF. Outcrops of the Bitter Ridge Limestone Member (Tbr) and the Muddy Creek gypsiferous member (Tmg) were only mapped in the hanging wall. The Tbr was only recently identified and mapped by Beard et al. (2007), as is shown in Plate 1. Large blocks of Cenozoic volcanic rocks (Tvr) are prominent in both the footwall and hanging wall and are intercalated within these units (Plate 1.)

Geologic mapping showed which units the SW FMF cuts or displaces in the field study area. There are few exposures of the SW FMF in which the units are well exposed

on both sides of the fault. Much of the inferred position of the SW FMF that was mapped was based on stratigraphic locations, major topographic changes, or is expressed as a series of faults.

Based on observations in the field and comparison with rocks mapped as the Muddy Creek Formation, I concluded that some of what had been previously mapped as the Tmc could in fact be Red Sandstone (Tr). This conclusion is based on previous work done in close proximity to this study area by Rittase (2007), which demonstrated that units that had previously been mapped as Tmc were in fact Tr based on tephrochronology dating. The unit previously mapped as Tmc in the field study area matches the description of Tr described by Rittase (2007) and is an unsorted to poorly sorted conglomerate that ranges from matrix supported to clast supported in some areas, with a matrix that consists of coarse to fine-grained angular sandstone and siltstone. Clasts can range in size from one centimeter to three meters in diameter. Bedding typically ranges from approximately 5-50 cm but in places can be meters thick. Clasts are composed of predominantly igneous material including basalt, megacrystic plagioclase (rapakivi) and granite, as well as quartzite. The unit also contains significant amounts of sedimentary clasts of sandstone and carbonate, as well as gneiss clasts. The description of the Tr, which was previously identified as Tmc, in the Rittase (2007) study is very similar to the unit previously mapped as the Tmc in this field study area. The Muddy Creek Formation is highly variable in southern Nevada (Bohannon, 1984; Langenheim et al., 2000; Hanson et al., 2005; Forrester, 2009). Although I attempted to find datable materials in the Tr, no radiometric dating was completed in this study. The assumptions I made to suggest that the unit in the field study area is Tr are: 1) low dip angles of bedding within the unit

indicative of little deformation and tilting (Bohannon, 1984), 2) interbedded conglomerate that includes volcanic and plutonic clasts (Scott, 1988), and 3) age constraints based on relative stratigraphic relationships. These assumptions do not conclusively identify this unit as Tr and it is possible that it is Tmc as previously suggested. The Tmc was previously proposed to be post Cenozoic deformation basin fill, but recently other authors have documented syntectonic deposition within the Tmc. The most current absolute age of the Tmc is based on tuffs and basalt flows and is approximately 8.5-4.1 Ma (Metcalf, 1982; Bohannon, 1984; Williams, 1996; Hanson et al., 2005). The Tmc in the FMB area was previously divided into two units: the traditional Tmc, as well as a more gypsiferous unit, the Tmg. Based on the assumptions listed above and the similarity of this unit to those that were documented by Rittase (2007) I chose to map the unit as Tr, not Tmc. Quaternary deposits in the field area were divided into active alluvium in modern washes (Qa); Quaternary deposits with significant petrocalcic development (Qp); and disturbed landfill deposits (Qd). Detailed unit descriptions are included in Plate 1. The implications of this interpretation will be discussed further in the conclusions and interpretations section of this report.

Geologic Mapping Discussion

Rowland et al. (1990) asserted that the Thumb and Bitter Ridge Limestone members were deposited in close proximity to the Gold Butte block prior to translation of the FMB. The interpretation of Rowland et al. (1990) is supported by the results of this study, which found large landslide blocks of Gold Butte affinity on top of, and in some cases, encased within the Thumb and Bitter Ridge units in both the hanging wall and the

footwall. Therefore, the main fault mapped in this project along the southwestern side of the FMB (called the FMF by previous workers) cannot be the main FMB-bounding fault for the entire history of motion of the fault because rocks on both sides of it have been transported from the Gold Butte area. The true FMB bounding fault must be located farther to the southwest (most likely buried) based on the presence of Gold Butte derived blocks in both the hanging wall and footwall (Fig. 6).

My mapping also places constraints on the timing of the FMF based on the relationship between units along the fault. The Thumb Member of the Horse Springs is cut by the FMF, therefore displacement on the FMF must have occurred post-deposition of the Thumb. The age of the Thumb Member is 13.9-16.2 Ma based on $^{40}Ar/^{39}Ar$ data from Beard (1996) and an upper age taken from a biotite of 13.9 Ma (Castor et al., 2000). The Bitter Ridge Limestone mapped in the hanging wall of the FMF, which is approximately 13.1 Ma (Castor et al., 2000), though not directly cut by the FMF in the study area is obviously offset from other outcrops of the Bitter Ridge Limestone that are mapped further to the northeast. Therefore, the SW FMF must have slipped sometime after 13.1 Ma. The Tr sits depositionally on all of the older units that it is in contact with and it overlaps the SW FMF is several places. Therefore, motion on the SW FMF ceased prior to deposition of the Tr, i.e., sometime prior to 8.5Ma (initiation of Muddy Creek deposition) and possibly as early as 12-10.6 Ma (the age of the Red Sandstone according to Rittase (2007)).

There are large angular clasts within the Tr all along the fault. Their presence indicates that the Tr was deposited close to significant relief and I infer that the Tr was deposited soon after the last displacement occurred on the fault. I also infer that the last

motion on the fault had normal sense offset and that it down-dropped the hanging wall to the southwest, thus creating proximal accommodation that became the site of Tr deposition. Although the Tr sits depositionally on top of the SW FMF and constrains the timing of motion on the fault, the Tr is cut by roughly N-S faults in at least two locations. The relationship between the N-S faults that cut the Tr and the older SW FMF are not clear although it is clear that they are younger than the SW FMF.

The Tmg unit of the Muddy Creek Formation in the map area is comprised of fine-grained homogenous gypsiferous sediments and was most likely deposited in an evaporative setting such as a playa. Due to the nearly flay-lying, fine-grained nature of the unit, the Tmg is interpreted as post-tectonic sedimentation. This provides additional support for the idea that tectonic activity along the SW portion of the FMF had stopped prior to Muddy Creek time. As previously mentioned the Tr unit differs from the Tmg in that it is far coarser and is comprised of angular clasts up to three meters in diameter proximal to the FMF; average clast size increases with proximity to the fault. Accordingly the Tr was potentially deposited soon after the last motion on the SW FMF due to the large clast size proximal to the fault and the angular nature of the clasts. The Thumb Member consists of siliciclastics, sandstones, siltstones, conglomerates and evaporates.

Fault Kinematic Data and Results

Major Fault Sets

Detailed geologic mapping paired with collection of kinematic data allowed for a more complete understanding of structural relationships in the field area. Following field

observation and recording of fault position and orientation, analysis of these data was done using the Stereowin 1.2 Stereonet program (Allmendinger, 2002) and three main fault sets were identified. The fault sets were classified based on: 1) location within the field area relative to what stratigraphic units were in the footwall and hanging wall of the fault, 2) the strike and dip of the fault, 3) cross-cutting relationships relative to other structural features. Two schematic cross sections were constructed to provide a pictorial representation of the stratigraphic and structural relationships, their location and orientation is shown in Figure 7, and the cross sections are shown in Figures 8a-b. Structural, stratigraphic and kinematic data from the field area are reported in Appendices I-II, and their location within the field area are labeled and shown in Plate 1. For the purposes of this paper, the fault sets are referred to as A, B, and C and their respective orientations can be seen in Figure 9.

The structural features that were consistent with previously mapped orientations of the SW FMF are represented by fault set A (Fig. 10). This fault set consists of five faults, has an average strike of 128°, and an average dip of 63° to the southwest. The faults were identified as being part of this fault set because of their respective orientations and location within the field along where the SW FMF had previously been mapped. Exposure of these faults is relatively poor due to burial and erosion. The faults are exposed within the Moenkopi Formation, Rainbow Gardens and Thumb Members of the Horse Spring Formation, volcanic rocks of Rainbow Garden, and the Red Sandstone.

Fault set B consists of 12 faults that have an average strike of 179° and an average dip of 67° to the west (Fig. 11). The faults strike north-south and are exposed within the

Kaibab Formation, Moenkopi Formation, Thumb and Rainbow Garden Members of the Horse Spring Formation, volcanic rocks of Rainbow Garden, and the Red Sandstone.

Fault set C is conjugate to fault set B, and is represented by three structures (Fig. 12). These faults have an average strike of 341° with an average dip of 73° to the east. The faults strike northeast-southwest and are exposed within the Thumb and Rainbow Garden Members of the Horse Spring Formation as well as the Red Sandstone.

Slickenlines and Mullions

Slickenline data were collected during fieldwork on seven separate fault surfaces. The slickenline data were plotted and analyzed using the Stereowin 1.2 stereonet program. Within the seven fault surfaces with slickenlines, two sets of conjugate faults were identified providing further information about relationships between fault sets regarding their age and relative sense of offset. All of the slickenline data and correlating fault orientations are in Appendix III.

Conjugate fault set one is exposed within the Rainbow Gardens conglomerate (Trc) and is shown in Figure 13. One fault is from group C, has an orientation of 349°, 79° E and has four slickenline measurements which indicate primarily normal sense slip with a minor component of oblique motion to the northeast. The conjugate fault is from group B, strikes 179°, dips 67° W and has six slickenline measurements associated with it that also indicate normal sense motion with minor oblique motion to the southwest.

A second set of conjugate faults is exposed within Trc conglomerate and is shown in Figure 14. One fault is from group C, has an orientation of 350°, 76° E and has three slickenline measurements which indicate primarily normal displacement with minor oblique fault motion to the east-southeast. The conjugate fault is from group B, strikes

186°, dips 70° W and has two slickenline measurements associated with it that also indicate fault motion was primarily normal with a minor component of oblique motion to the west.

Additional faults crop out that have slickenlines on the exposed surface including slickenlines on the SW FMF from fault set A, as well as slickenlines on faults within set B. Slickenlines measured on the SW FMF fault were located on a surface that strikes 162° and dips 80° to the southwest and is exposed between Trc and Rainbow Gardens red sandstone (Trr). On Figure 15a the strike of the fault plane is taken from aerial images because the field exposures were limited. This fault surface has eight slickenlines as well as mullions exposed and they indicate primarily normal sense displacement with minor oblique motion to the southwest (Fig. 15b). Two additional minor faults have slickenlines on the exposed fault surface. An additional fault from set B strikes 184°, dips 51° W (Fig. 16) and juxtaposes the Thumb Gypsum-rich sequence (Ttg) and the Thumb Conglomerate (Ttc). This fault has three slickenlines associated with it that indicate oblique fault motion directed to the northwest. The final fault with slickenlines is from group B, and strikes 2° and dips 86° to the west (Fig. 17). There is only one slickenline on this fault surface and it indicates oblique motion to the southeast.

Fault Kinematic Discussion

I identified three main fault sets and determined their temporal relationship relative to each other and the results bear on the structural evaluation of the area. The dominant extensional direction is west-southwest, with some component of a conjugate motion directed to the east-southeast.

Fault set A represents the main FMF and data from slickenlines on the surface of the faults indicate extension was oriented along a SW-NE axis. Slickenlines taken from fault surfaces in fault set B indicate dominantly oblique motion to the west. Out of 12 slickenlines measured, 11 indicate westward motion, while only one indicates motion to the east. Of the slickenlines that indicate motion to the west, motion to the southwest occur most frequently (n=six) followed by northwest directed slickenlines (n=three), and strictly west-directed motion (n=two). Fault set C represents a conjugate fault set, and slickenlines record fault movement directed generally to the east, with some slickenlines indicating northeast as well as southeast directed movement. None of the fault sets cross-cut each other which allows for the possibility that all fault motion was synchronous. Based on kinematic data and analysis, the primary extensional axis is NNE-SSW, with a minor axis oriented WNW-ESE (Fig. 18). In summary, the vast majority of kinematic data record normal sense offset.

Volcanic and Igneous Rocks Data and Results

Basaltic Intrusions

As previously mentioned in the geologic mapping portion of the results section, volcanic units are exposed on both the hanging wall and footwall sides of the SW FMF. In the southeastern part of the field area within the footwall (northeast side of the fault) the intrusive porphyry member (Tvr) of the volcanic rocks of Rainbow Garden are demonstrably intrusive in some locations and are surficial basaltic bodies in other places. These basaltic units lie stratigraphically above, below, and within the Thumb Member of the Horse Spring Formation. The units are sometimes individual flows that are

intercalated within Thumb beds, while others crosscut bedding in the Thumb Member. Farther north in the field area, similar deposits are mapped within the Thumb Member in the wash on the north side of the road into Rainbow Gardens (Plate 1). These basaltic bodies are intrusive, as they cross cut bedding and have clasts of the Thumb Member sandstone, siltstone and conglomerate unit (Tht) as xenoliths. Unusually discolored rocks were mapped in close proximity to igneous rocks and I have interpreted them to be thermally altered.

Numerous volcanic ashes are exposed within the field area, most of them within the Tr and Thumb Members. These exposures consist of altered, green to white beds of volcanic ash that had been reworked and are gypsiferous. Six thin sections were made and upon subsequent petrographic analysis, unaltered biotites were found within several samples. Very small sanidines were also found, but ultimately the ashes were determined to be unsuitable for further analysis using $^{40}Ar/^{39}Ar$ geochronology because the phenocrysts were too small. Original volcanic glass had converted to clay minerals making them unsuitable for tephrochronology.

Volcanic and Igneous Rocks Discussion

The volcanic and igneous rocks within the field area are within both the hanging wall and foot wall, and are mostly located within the Thumb Member. These units are most likely coeval with the River Mountains Volcanic rocks based on their location within the Thumb stratigraphy. Castor et al. (2000) dated this unit at 13.8-12.0 Ma by $^{40}K/^{39}Ar$ ages on biotite and hornblende. This geochronological evidence supports the assumption that the FMB was adjacent to the River Mountains by approximately 13 Ma,

however, they are geochemically different (personal communication E.I. Smith, 2010). These basaltic dikes are coeval with other exposures within the Thumb Member which are exposed along Lake Shore Drive (personal communication E.I. Smith, 2010).

Provenance Data and Results

Conglomerate Clast Counts

Conglomerate clast counts were conducted along three transects that generally run perpendicular to the SW FMF. The location of transects and the clast counts (Fig. 19), were chosen to represent the lateral variation within the field area. Multiple clast counts were taken along each transect to accurately represent the proximal to distal variation in conglomerates adjacent to the fault. All of the clast counts were taken within the Red Sandstone (Tr) to ensure continuity in the clast count data as well as to determine the compositional differences. All of the clast count data are presented in Appendix IV.

The Rainbow Gardens wash transect (RG wash) is located in a wash with excellent exposure of Tr just north of the RG wash (Fig. 19). Five clast counts were taken and a visual representation of the averages taken from these clast counts is shown in Figure 20. The percentage of igneous clasts generally increased with distance away from the SW FMF, and ranged from 52-69% of the clasts. The igneous component was dominantly plutonic, intermediate-composition clasts, and megacrystic plagioclase intrusive clasts (rapakivi granite). The volcanic component of the RG Wash was higher than in the other transects and comprised 29% of the total clasts. These volcanic clasts are vesicular basalt clasts. The sedimentary clasts within the RG wash were highly variable and did not have an overall trend, ranging from approximately 19-42% of the clasts.

Sedimentary clasts were dominated by red sandstone and red brecciated conglomerate clasts, and had the least amount of carbonate clasts of all three transects. The metamorphic clasts within the RG wash represent the smallest percentage of clasts, and also do not represent any kind of trend, ranging from 3-11 % of the total clasts. The metamorphic clast types were all gneissic in composition.

The second transect of conglomerate clast counts is located within the middle wash of the field area, and its position and the distribution of the clast counts are shown in Figure 21. Four clast counts were taken to represent this transect as the Tmc is less well exposed than in RG wash (Fig. 19). The igneous component of the clast counts were relatively consistent along this transect, with average compositional percentages ranging from 38-42%. These clasts were dominantly plutonic, intermediate-composition clasts with a small portion of megacrystic plagioclase intrusive clasts. The sedimentary clasts within the middle wash comprised 39-48% of the clasts within the clast counts. This transect had the greatest percentages of red sandstone clasts (25%) as well as the greatest amount of carbonate clasts (12%) of all three transects and has a relatively large component of red brecciated conglomerate. The metamorphic clasts within the middle wash represent 11-21% of clasts and are gneissic in composition.

The transect in the farthest southeastern part of the field area is the southern wash transect and only three clast counts were taken within it as the exposure of the Tmc is relatively poor (Fig. 19, Fig. 22). The percentage of igneous clasts decreased as the position moved farther away from the SW FMF, ranging from 42-51%. The igneous clasts were almost all plutonic, intermediate-composition clasts, which represented 42% of all of the clast types. The sedimentary clasts within the southern wash transect

consisted of red sandstone and significant amounts of carbonate and ranged from 25-32% of the overall clast compositions. The metamorphic component of the clast counts in the southeastern wash was the highest of all three transects, ranging from 19-25%, and were gneissic in composition.

The conglomerate clast counts from all three transects were directly compared to each other in order to allow for interpretation of the differences in composition (Figs. 20-22). These three sections vary laterally along the SW FMF, but are internally consistent within each transect.

Paleocurrent Data

Paleocurrent indicators that record paleoflow directions were measured at eight locations in the field area (Fig. 23). Paleocurrent indicators were measured in the three washes that conglomerate clast counts data were taken from. Indicators were taken in the Red Sandstone from imbricated clasts within interbedded conglomerates and were plotted on rose diagrams using the Allmendinger 1.2 Stereonet program. Overall, the paleocurrent indicators have a mean vector of 202°, indicating paleoflow was directed to the south-southwest (Fig. 24).

Provenance Discussion

The combination of conglomerate clast counts and paleocurrent data supports a derivation from sediment source areas that are directly across the SW FMF. The data are consistent with detritus being derived from the footwall and being shed directly (south-southwest) across the SW FMF into the basin. Conglomerate clast count data are highly variable laterally, but are internally consistent within each wash and overall, all three

transects had clasts compositions that represented provenance source areas adjacent to them, to the north-northeast. The RG transect contained the highest amount of volcanic clasts. This makes sense given that there are large outcrops of both Tvr and Ttb, the two main volcanic components of the field study area just to the northeast of the clast count site (Figure 25). Within the middle wash, red sandstone and carbonate clasts had the highest compositional percentages. This coincides with an area north of the fault that contains abundant Trl (Figure 25). All three washes have a significant amount of metamorphic gneissic clasts with Gold Butte affinity. The nearest Gold Butte source areas are to the north-northeast within the Frenchman Mountain block. An interpreted northeast to southwest transport direction inferred from the clast count data are supported by the paleocurrent data which indicates south-southwestern directed paleoflow.

If I had found that the SW FMF cuts the Tr, then the relatively compartmentalized basin stratigraphy recorded in this project and the determination that lithologies in the Tr correlate with source area directly across the FMF as determined by paleoflow indicators and the clast composition data would suggest normal fault offset along the FMF. In that scenario, detritus from the north-northeast was linked through time to the same part of the adjacent basin, without the basin fill experiencing any lateral movement (Fig. 25). However, because the Tr was found to be post-tectonic, the provenance and paleocurrent data documented here do not inform us as to the sense of motion on the SW FMF. Rather, they simply reflect direct transport of sediment from the elevated footwall of the SW FMF across the now-inactive SW FMF into the topographically lower hanging wall on the southwestern side of the fault. The fact that the hanging wall was lower than the foot wall does suggest that the SW FMF experienced normal sense, down to the SW motion.

CHAPTER 6

INTERPRETATIONS

Geologic mapping of field relationships, structural, stratigraphic, kinematic and provenance data have allowed for further interpretation of the motion, relative timing, and the significance of the SW FMF as well as potential identification of the FMB-bounding fault. Based on the new data, I speculate and offer additional hypotheses to explain the geology of the field study area. While these ideas are highly speculative, discussion of potential hypotheses may stimulate interest in future research and offer perspectives on the Lake Mead region geology:

1) Cenozoic units are exposed and have been mapped in both the hanging wall and the footwall blocks of the SW FMF. It is well-established that a portion of these units were deposited in close proximity to Gold Butte prior to the FMB being translated to its current position (Rowland et al., 1990). Therefore, based on the fact that these units (Ttb, Tht, Thb) occur within the hanging wall and the footwall of the FMF, I conclude that the SW FMF is not the FMB-bounding fault. In addition to this, the Tr overlaps the SW FMF and is not cut by the fault and thus the SW FMF ceased moving prior to deposition of the Tr. It does appear that the Tr was deposited soon after the last motion on the FMF. This is supported by the coarse-grained proximal alluvial characteristics of the Tr and the presence of large angular clasts proximal to the SW FMF. Given that the fault that was previously mapped as the FMF is not the block-bounding fault, I hypothesize that the actual FMB block-

bounding fault is located farther out into the basin towards the southwest, as is shown in Figure 6.

2) Based on fieldwork and subsequent analysis I have concluded that the FMF is mostly likely a series of normal faults that can be divided into three groups: the "main" fault group which is northwest-southeast striking and southwest dipping (A), a secondary set of faults striking nearly north-south and dipping to the west (B), and a third set conjugate to set B which is striking northeast-southwest and dips to the east (C) (Fig. 9). In map view, a NW-SE striking feature separates higher topography from lower topography, and this has been identified in the past as the FMF. However, instead of this being one major structure, I propose that the combination of normal fault motion of these conjugate fault sets and subsequent erosion has caused it to appear as if there has been major strike-slip offset. In my hypothesized scenario, post-faulting erosion of the paleosurface material has created an apparent strike-slip offset sense in map view, but in fact is a normal fault (Fig. 26). However, these observations are not conclusive and I cannot rule out an overall strike-slip sense of motion for the FMF.

3) Structural and kinematic relationships in the field imply normal fault motion as indicated by: 1) the presence of vertical and sub-vertical slickenlines on fault surfaces; and 2) a lack of both structural and stratigraphic evidence that would suggest strike-slip motion. Although the slickenline and mullion data predominantly point towards normal sense offsets, these types of data always

indicate the last sense of motion on faults and thus earlier offsets that had a different sense can be overprinted by the last features.

4) Structural orientation and identification of the fault sets indicate that fault motion of all three fault sets occurred synchronously, as no field observations indicate any cross-cutting relationships of the fault sets. My data support the proposed extensional directions suggested by previous authors, and ultimately indicate the principle extensional axis oriented NNE-SSW and a minor axis oriented WNW-ESE shown in Figure 18.
5) My mapping of the Red Sandstone has possible implications for how researchers view the Tr. Further research and comparison of the Tr within the field study area to other nearby Tr exposures indicate that what has previously been mapped as the Muddy Creek Formation could in fact be the Red Sandstone (Rittase, 2007).
6) All previous researchers have referred to the fault that bounds the NW, W, and SW margins of the FMB as the FMF. My data clearly show that offset along the SW portion of this fault had ceased prior to deposition of the Tr. Given that the western portion of the FMF (at the western base of Frenchman Mountain) offsets Quaternary units, it is clear that if these two fault segments were linked in the past that they no longer are not linked and have not been linked for the past 8-12 million years. This has important implications for calculated magnitude estimates for the western FMF given that magnitudes are linked to fault length.

Based on the data generated in this study, it is possible to determine which previously discussed models proposed by other workers these data are most consistent with. My data are mostly consistent with models that propose extension oriented principally to the SSW-NNE, such as Anderson (1971), Bohannon (1979), as well as Weber and Smith (1987). Because parts of the FMF are located along the basin edge of the Las Vegas Valley, as previously discussed, there are various models for how the FMF fits into the larger picture of the development of the Las Vegas Valley. Langenheim et al. (2001) and Campagna and Aydin (1994) both evoke a pull-apart model for the formation of the Las Vegas Valley, but neither dealt definitively with the sense of offset of the SW FMF. The geometries of the fault sets in the Langenheim et al. (2001) model closely resemble the fault sets identified in this study: the fault planes strike NNW-SSE and SSW-NNE. Based on the data generated in this study, I hypothesize that the SW FMF and the FMB-bounding fault are part of a system of normal faults whose interaction has resulted in the formation of the Las Vegas Valley. Furthermore, my hypothesized location of the FMB-bounding fault proposed in this study is consistent with the geophysically inferred strand of the LVVSZ imaged by Langenheim et al. (2001).

This study has shown that the method of using basin structural and stratigraphic mapping techniques, paired with kinematic and provenance analyses can be a powerful tool in constraining the motion and timing of a fault. While my results and interpretations show that the actual FMB-bounding fault is likely buried in the Las Vegas Valley and are not absolutely conclusive regarding the movement of the master fault, the exposed structures give some insight into the possible location and significance of the fault. If the structures exposed on the surface are any indication of the FMF's movement,

I propose that the SW FMF is a normal fault that possibly has a component of oblique motion.

APPENDIX I

Figures

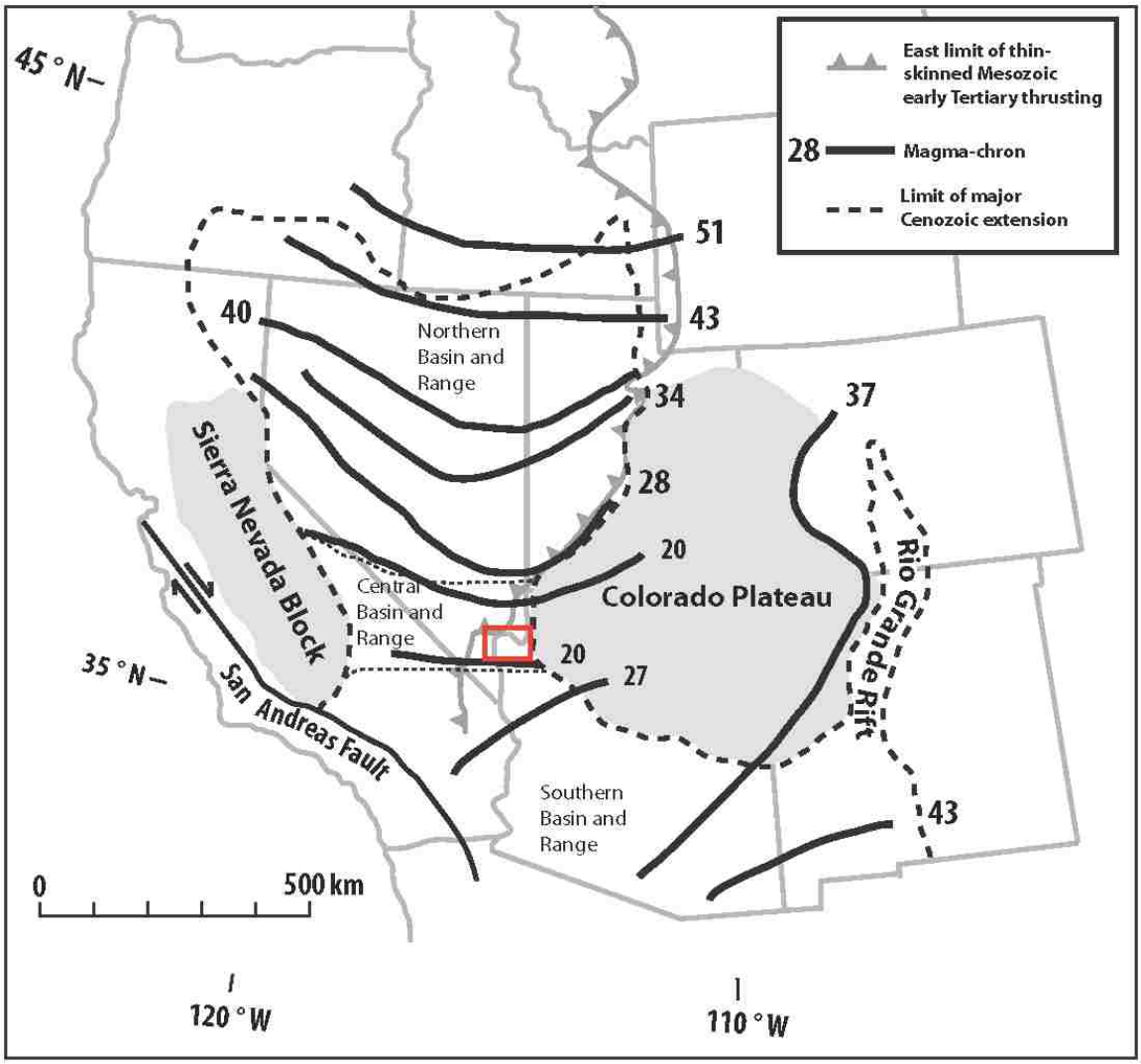

Figure 1. Map of western North America, Basin and Range province within the United States, labeling the Northern Basin and Range, Central Basin and Range and Southern Basin and Range. The field area is located within the red box (modified from Faulds et al., 2001).

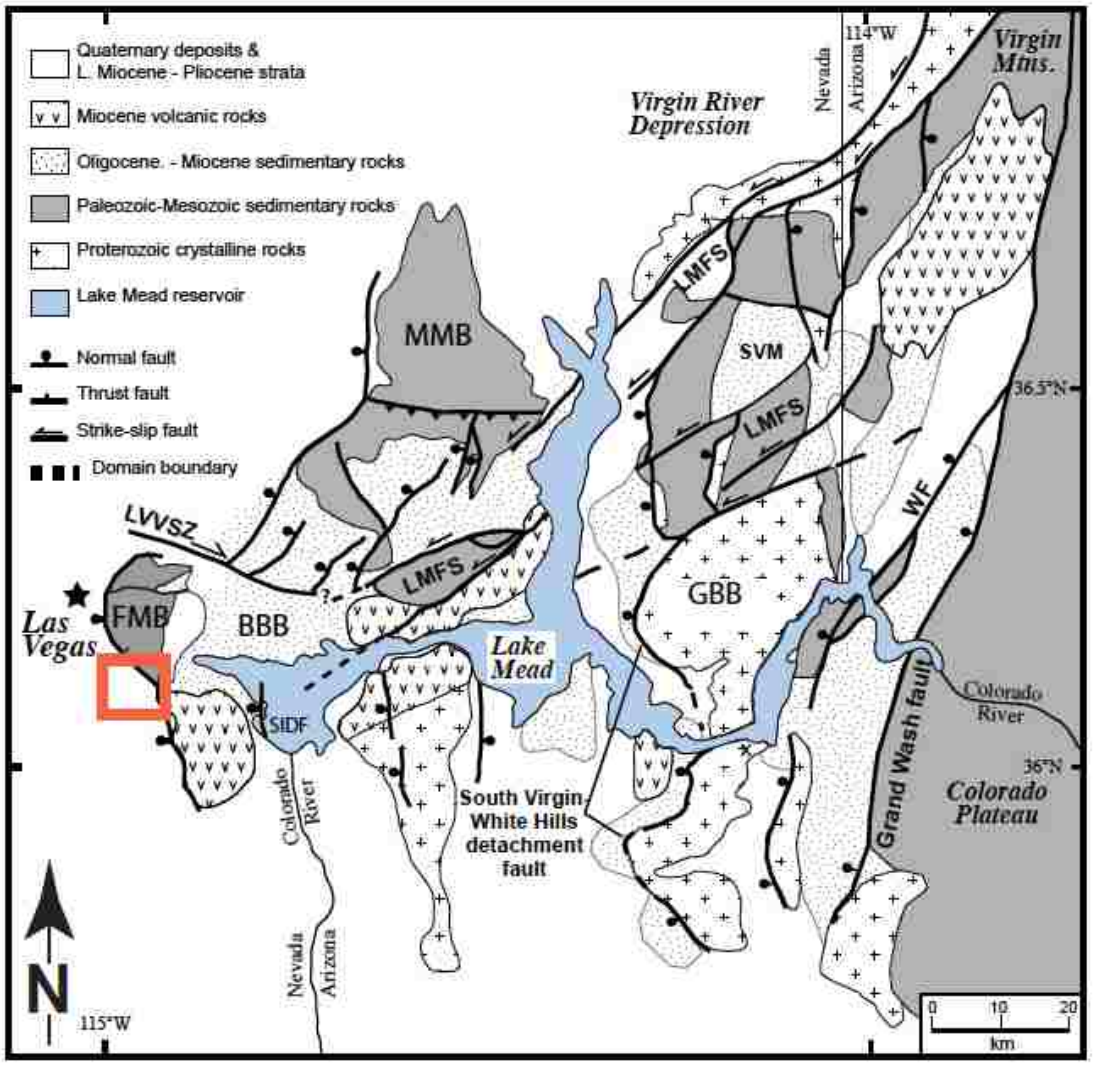

Figure 2. Lake Mead Regional geology, features shown are: Las Vegas Valley Shear Zone (LVVSZ), Lake Mead Fault System (LMFS), Saddle Island Detachment Fault (SIDF), Frenchman Mountain Block (FMB), Muddy Mountains Block (MMB), Boulder Basin Block (BBB), Gold Butte Block (GBB) (modified from Lamb et al., 2010).

Figure 3. Location map of Frenchman Mountain field study area outlined by the red box in Figure 2, outside of Las Vegas, NV. Features shown are: Las Vegas Valley Shear Zone (LVVSZ), Frenchman Mountain Fault (FMF), Munitions Fault (MF), Boulevard Fault (BF), and Dry Wash Fault (DWF).

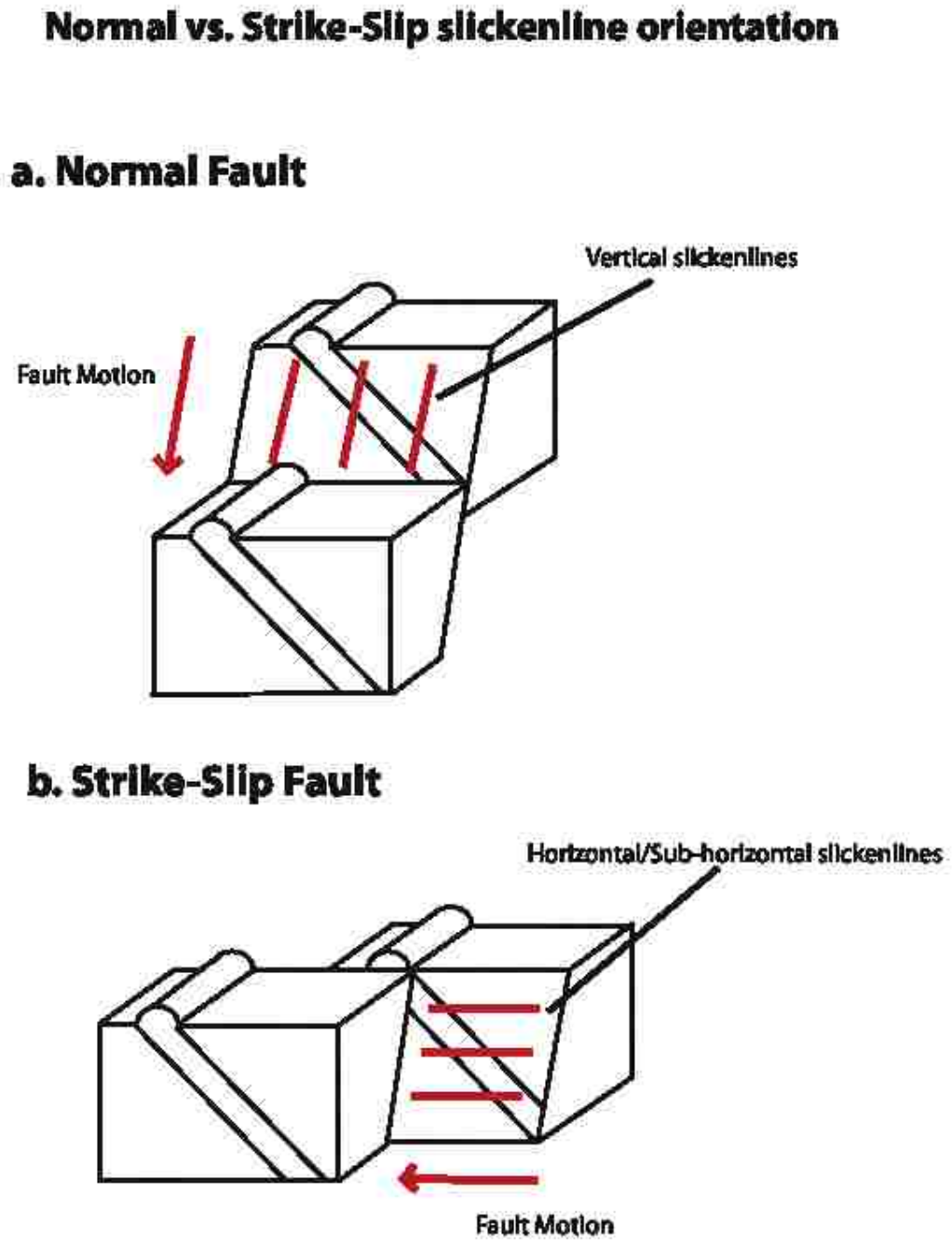

Figures 4a and b. Schematic slickenline diagram showing hypothetical slickenlines in the case of normal versus strike-slip scenarios. In the case of a normal fault (a), slickenlines would be vertical or sub-vertical (shown in top figure), conversely if the fault is a strike-slip fault (b) the fault surfaces would have horizontal or sub-horizontal.

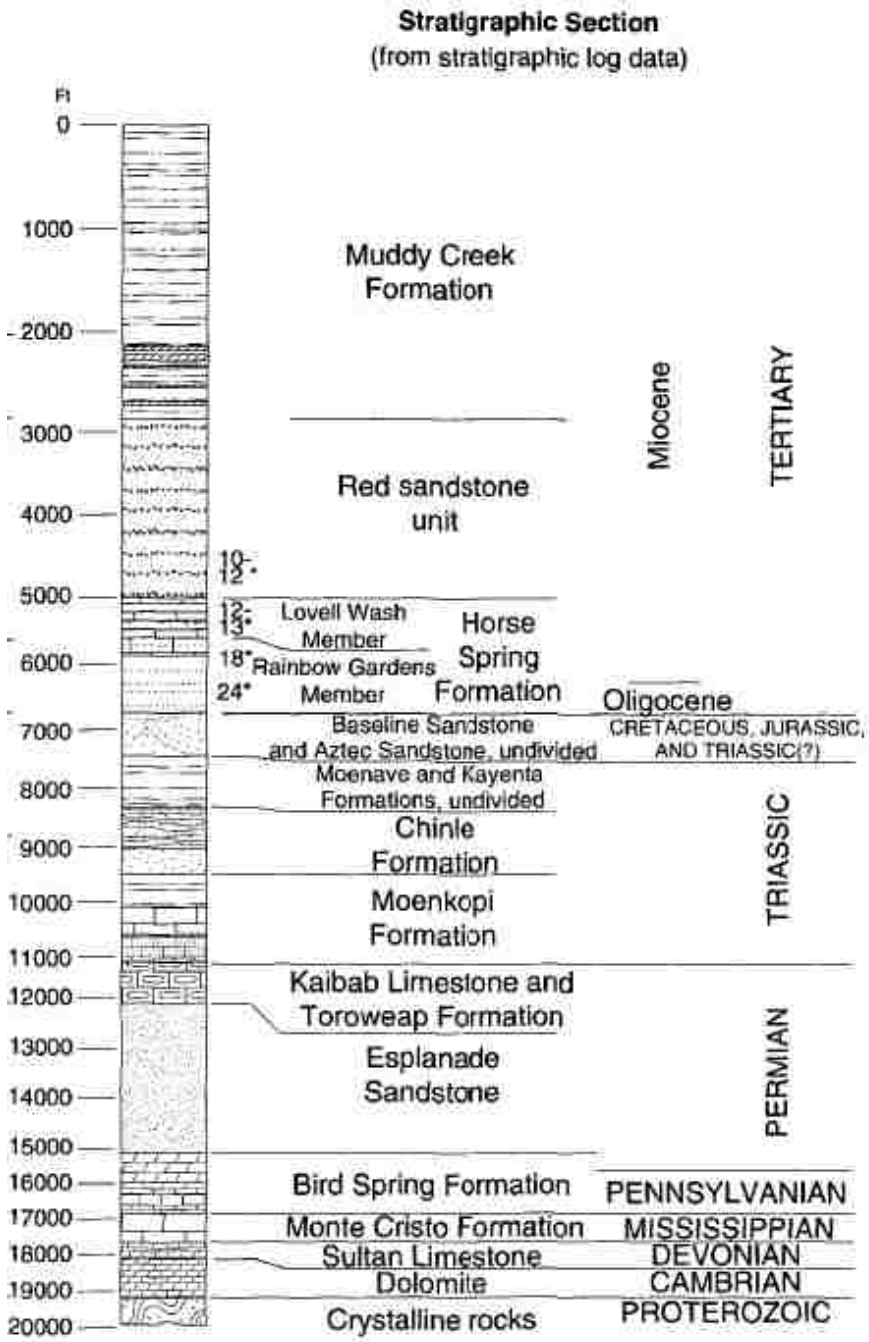

Figure 5. Stratigraphic column from the Mobil Oil Virgin 1A test well at Mormon Mesa, stratigraphy is the same as that exposed in the field area. Stratigraphic section shows stratigraphy based on well data (modified from Bohannon et al., 1993).

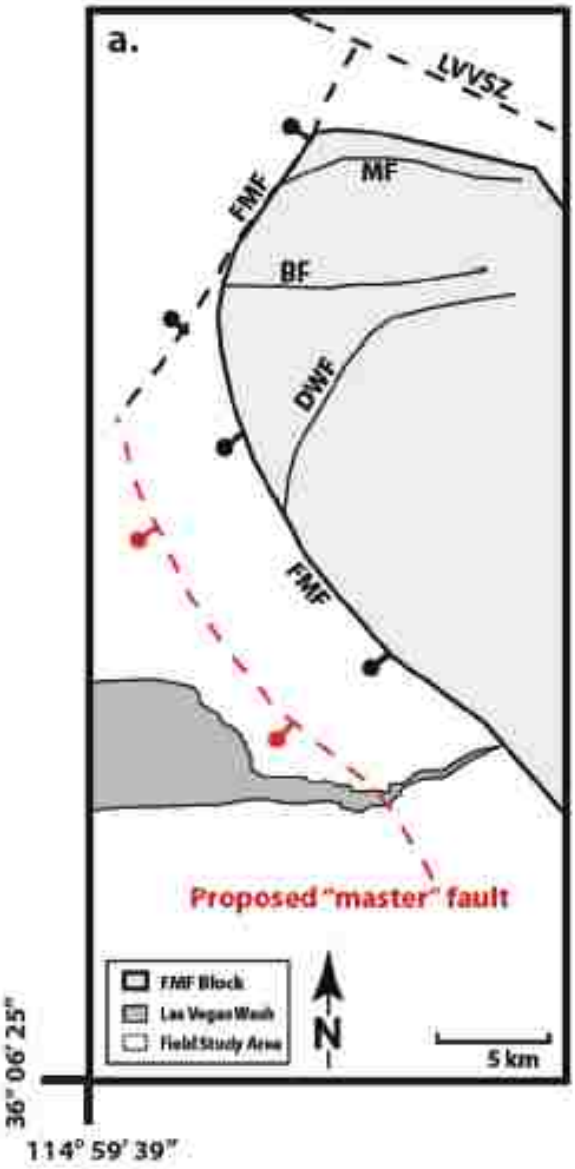

Figure 6. Interpretive figure showing the possible location of the proposed "master" fault shown in red, located to the southwest of the current FMF. Features shown are: Las Vegas Valley Shear Zone (LVVSZ), Frenchman Mountain Fault (FMF), Munitions Fault (MF), Boulevard Fault (BF), and Dry Wash Fault (DWF).

Figure 7.

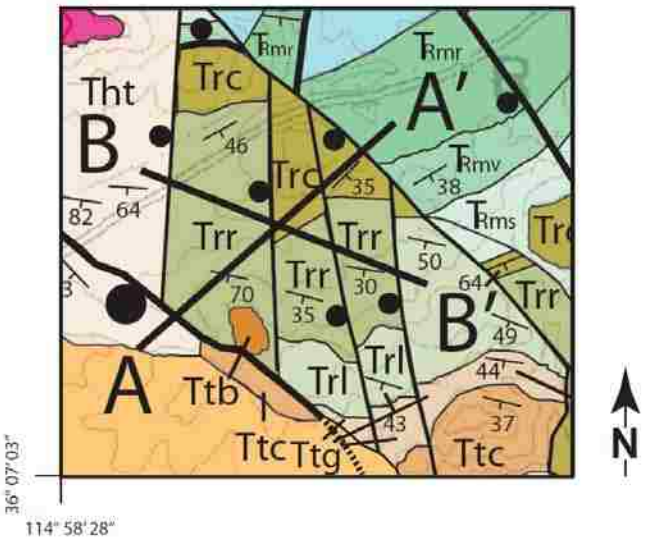

Figure 8a and b.

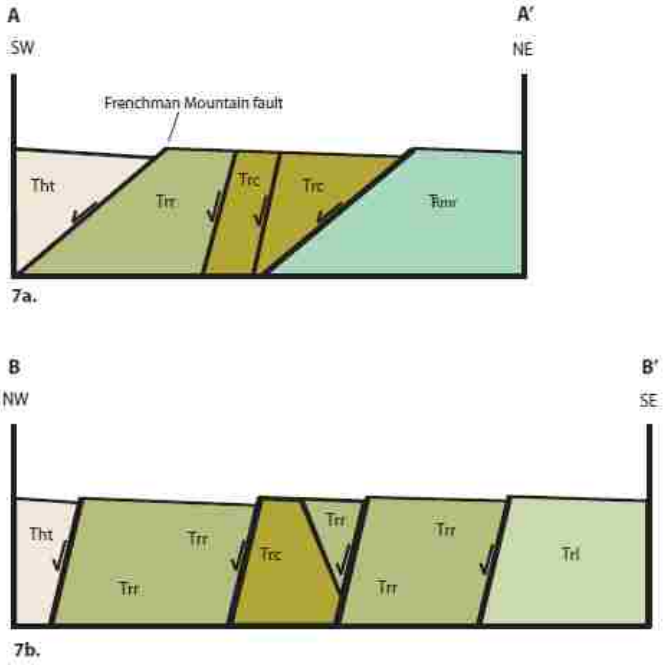

Figures 7 and 8a-b. 6) Location of schematic cross sections within field study area, location of black box is shown in Figure 6. 7a) Cross section A-A', cross section is schematic and not to scale, 7b) Cross section B-B', cross section is schematic and not to scale, dashed lines indicate schematic conjugate fault sets. See Plate 1 for units key.

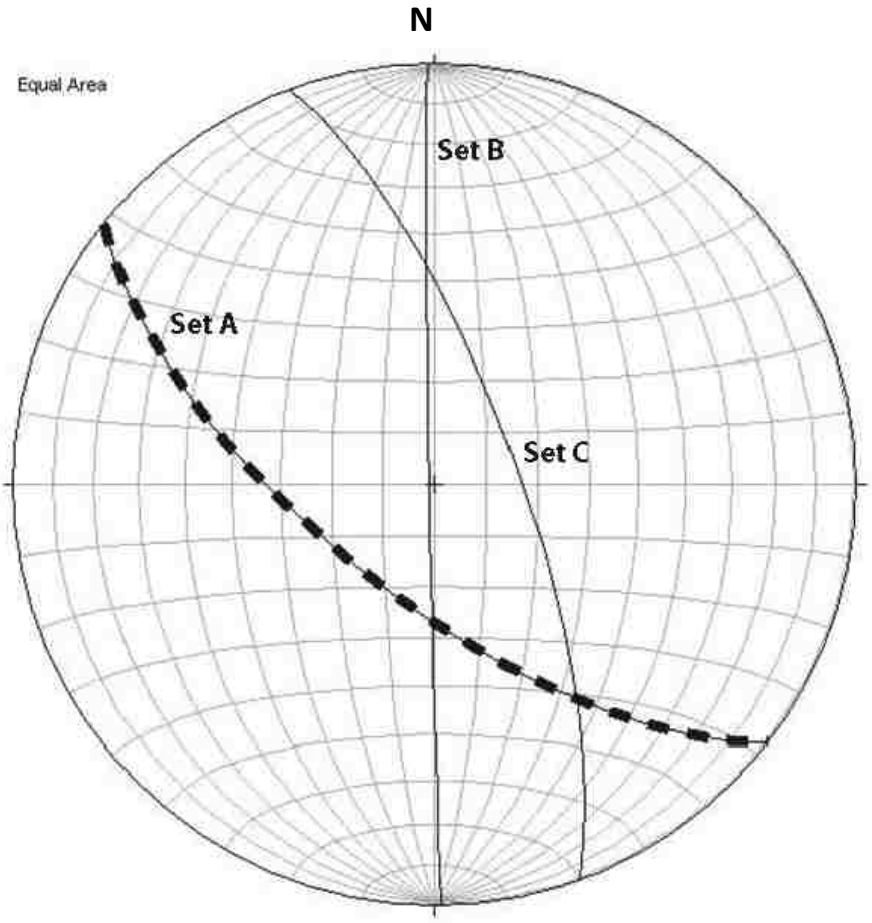

Figure 9. Stereograph showing the main fault sets, each fault set is represented by a single fault plane that averages all of the faults within the set. The “main” fault set (A) that represents the FMF is shown in the thick dashed line. Stereowin by Allmendinger (2002) was used to generate this and all following stereographs.

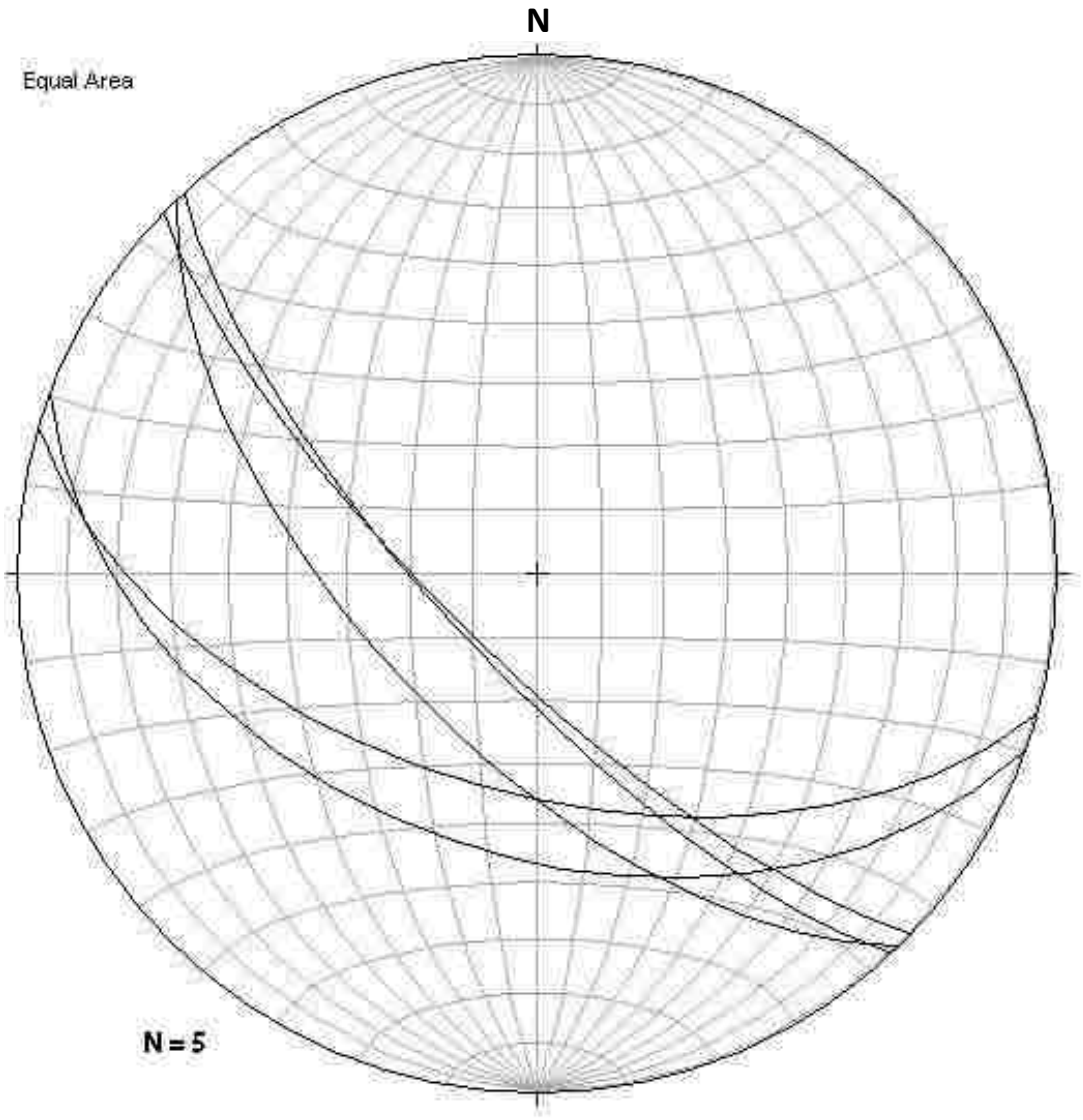

Figure 10. Stereograph of fault set “A”. Faults strike northwest-southeast and dip to the southwest.

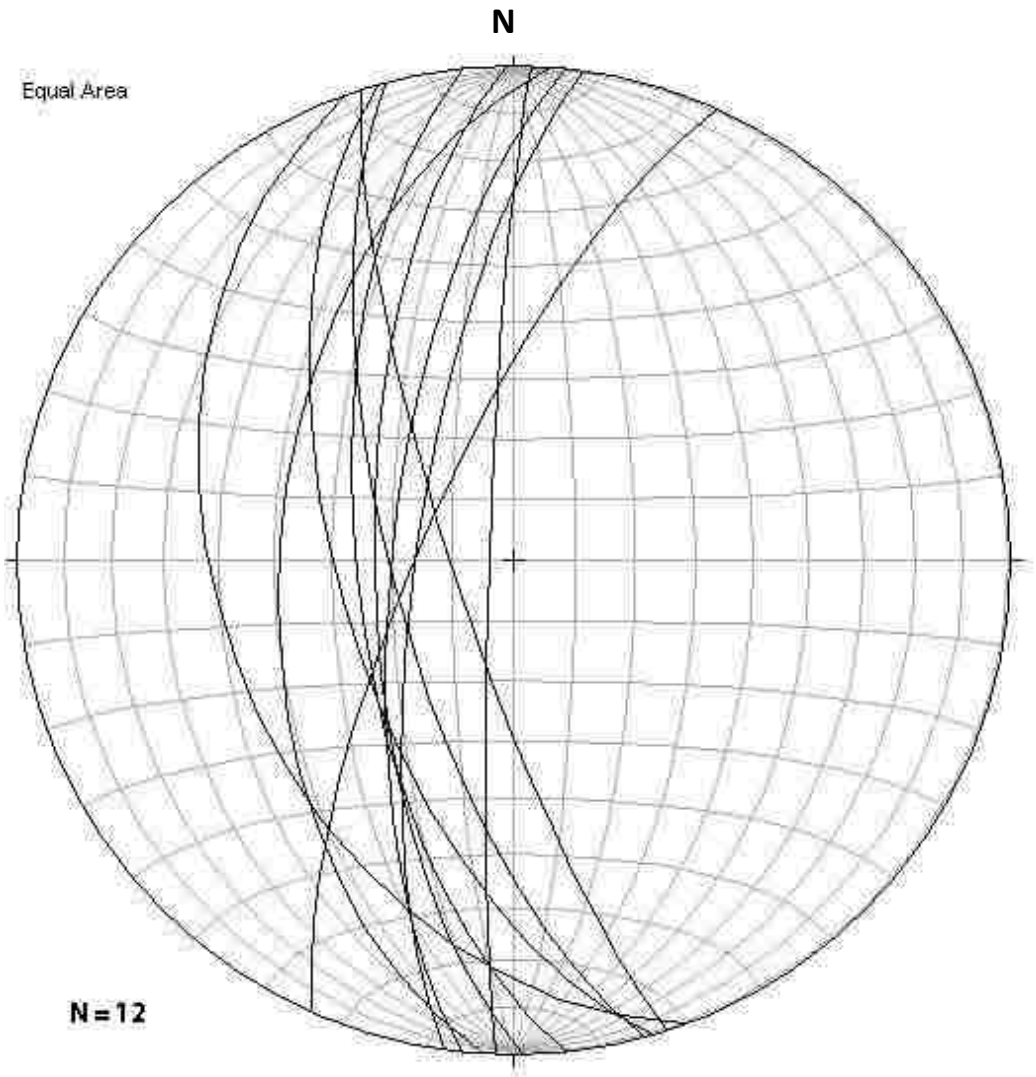

Figure 11. Stereograph of fault set “B”. Faults strike north-northwest to south-southeast and dips are to the west.

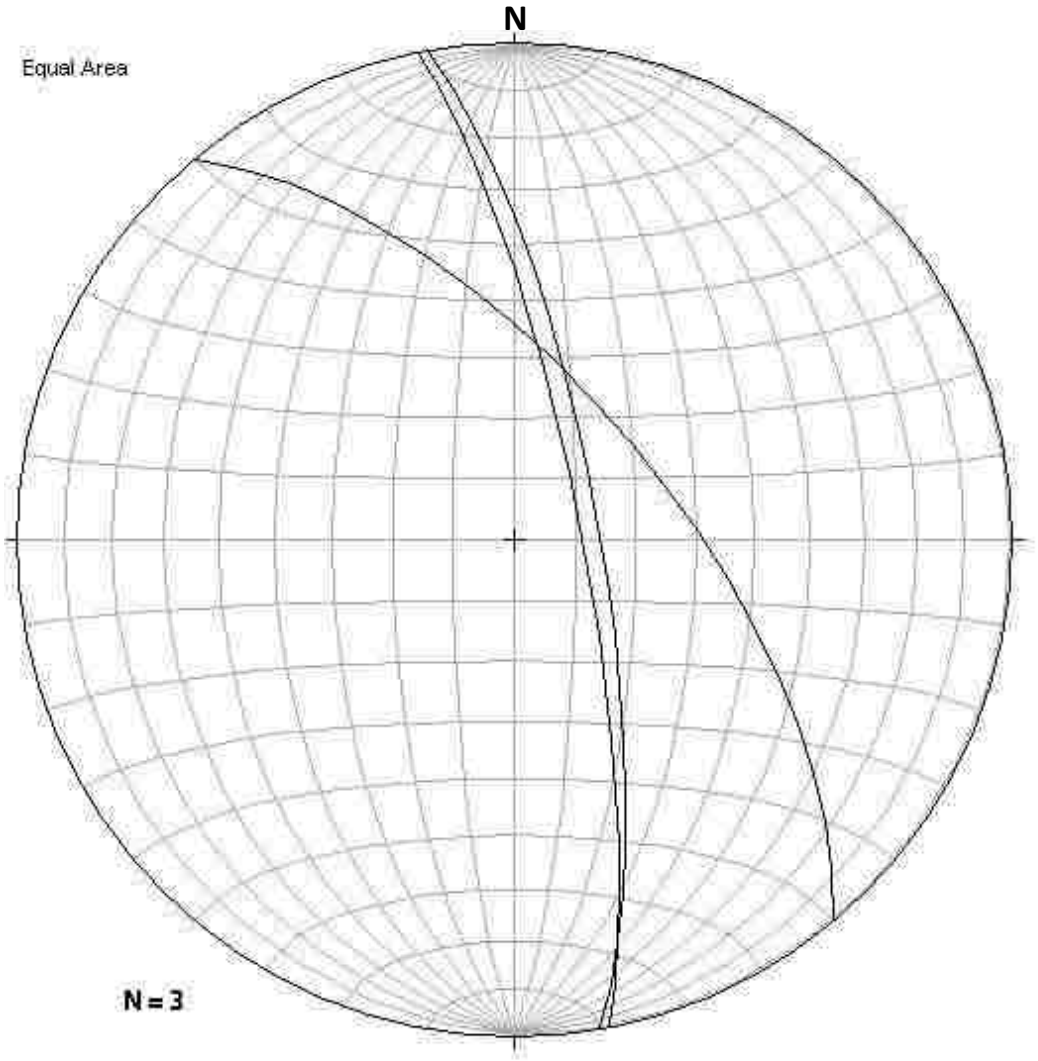

Figure 12. Stereograph of fault set “C”. Faults strike north-northwest to south-southeast and dip to the NE.

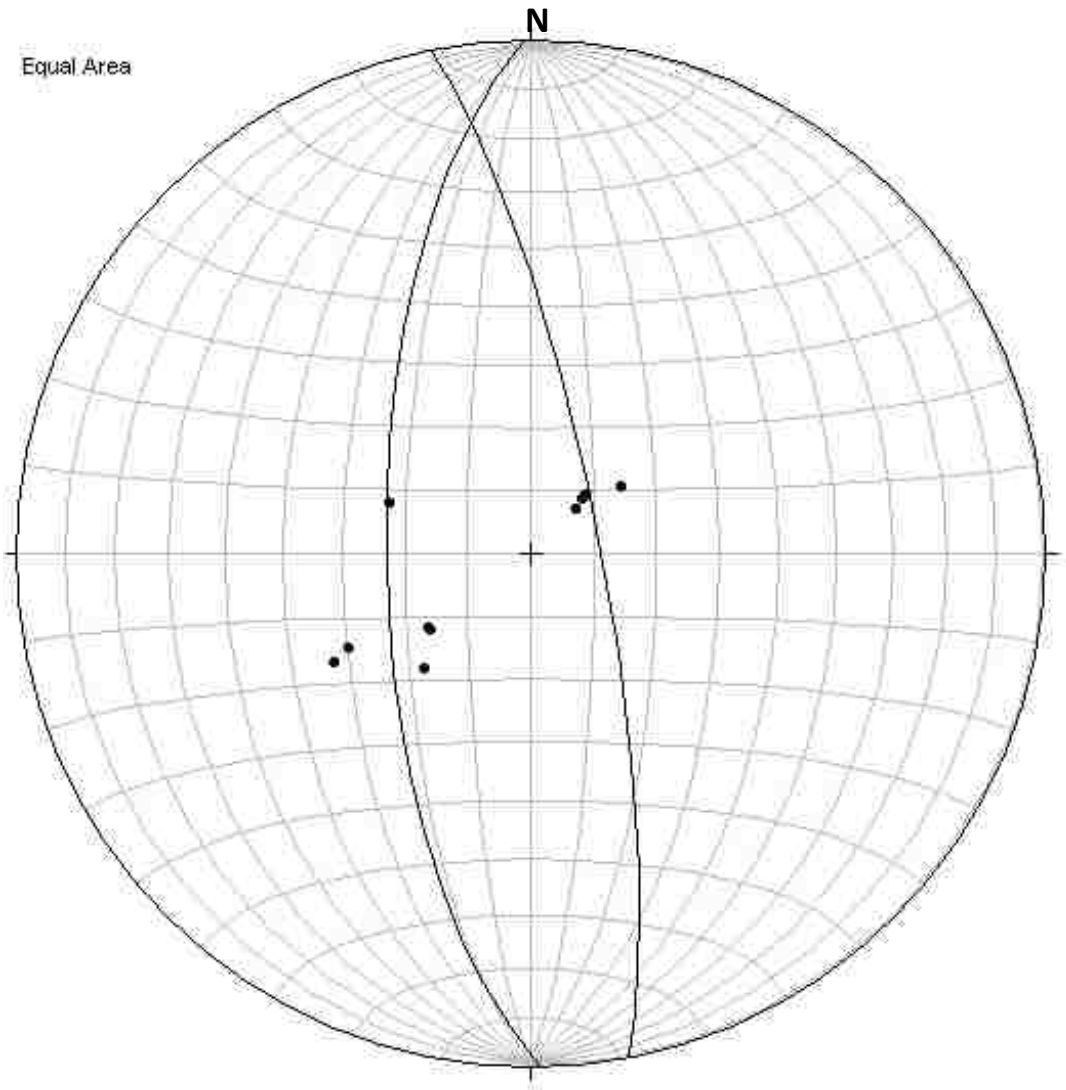

Figure 13. Stereograph of conjugate fault set one, plotted with corresponding slickenlines.

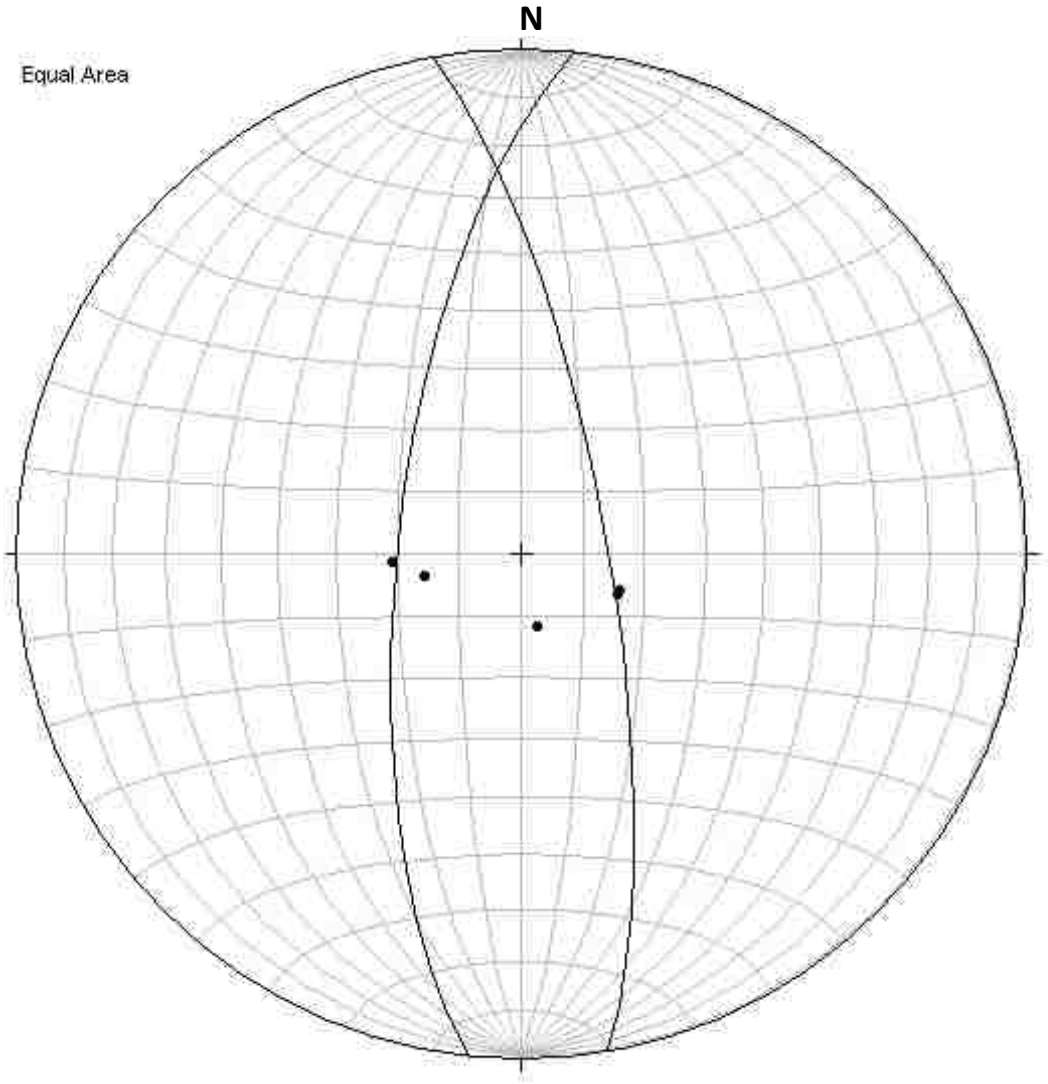

Figure 14. Stereograph of conjugate fault set two, plotted with corresponding slickenlines.

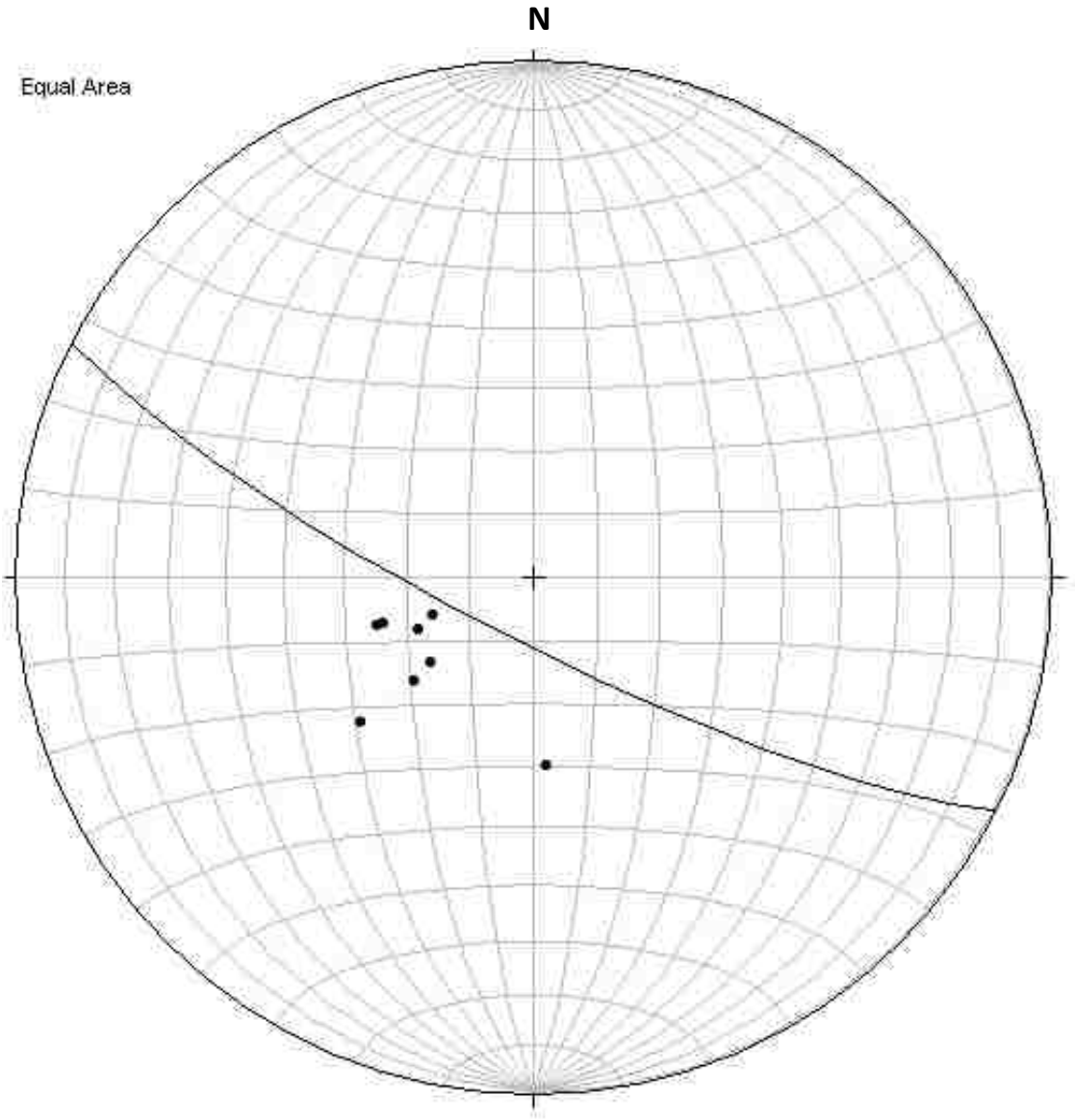

Figure 15a. Stereograph plot of main FMF fault surface with slickenlines. Fault plane orientation is an estimated approximation based on hypothesized fault location and orientation. The mismatch between the slickenline data and the fault plane suggests that the fault dip may be less steep than what was estimated.

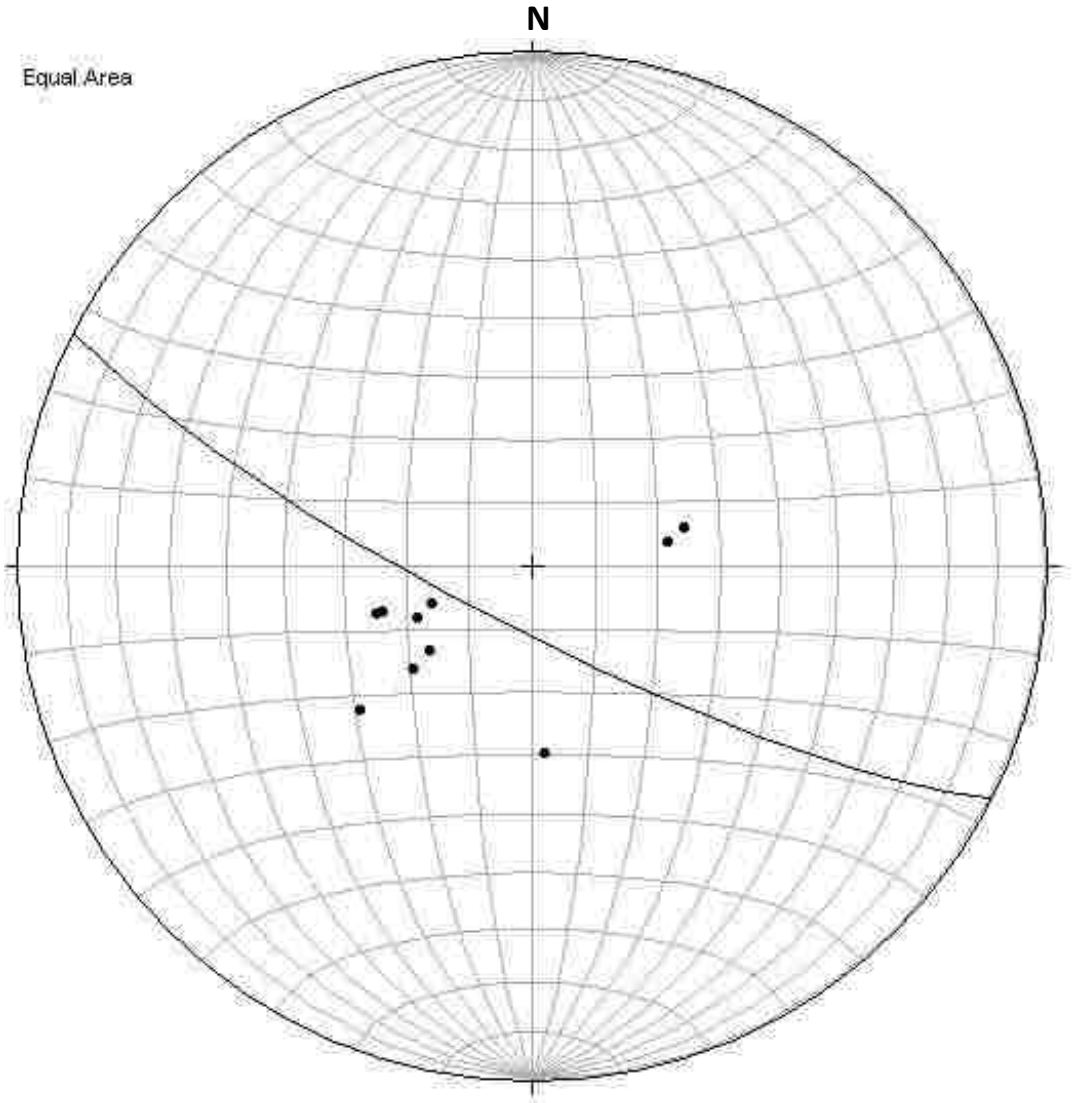

Figure 15b. Stereograph of main FMF fault surface with slickenlines and mullions.

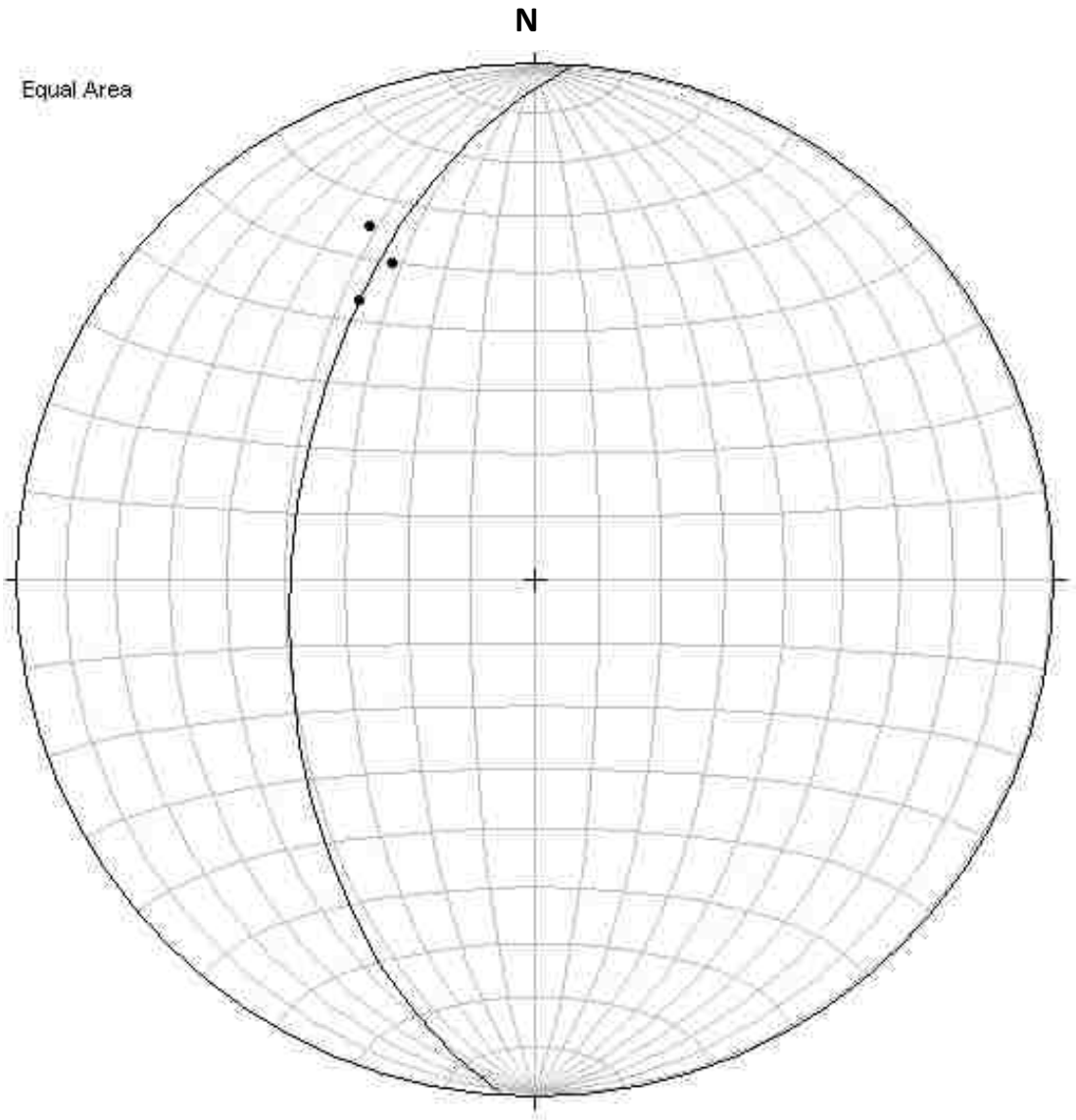

Figure 16. Stereograph with fault oriented 184°, dipping 51° and slickenlines from fault set B.

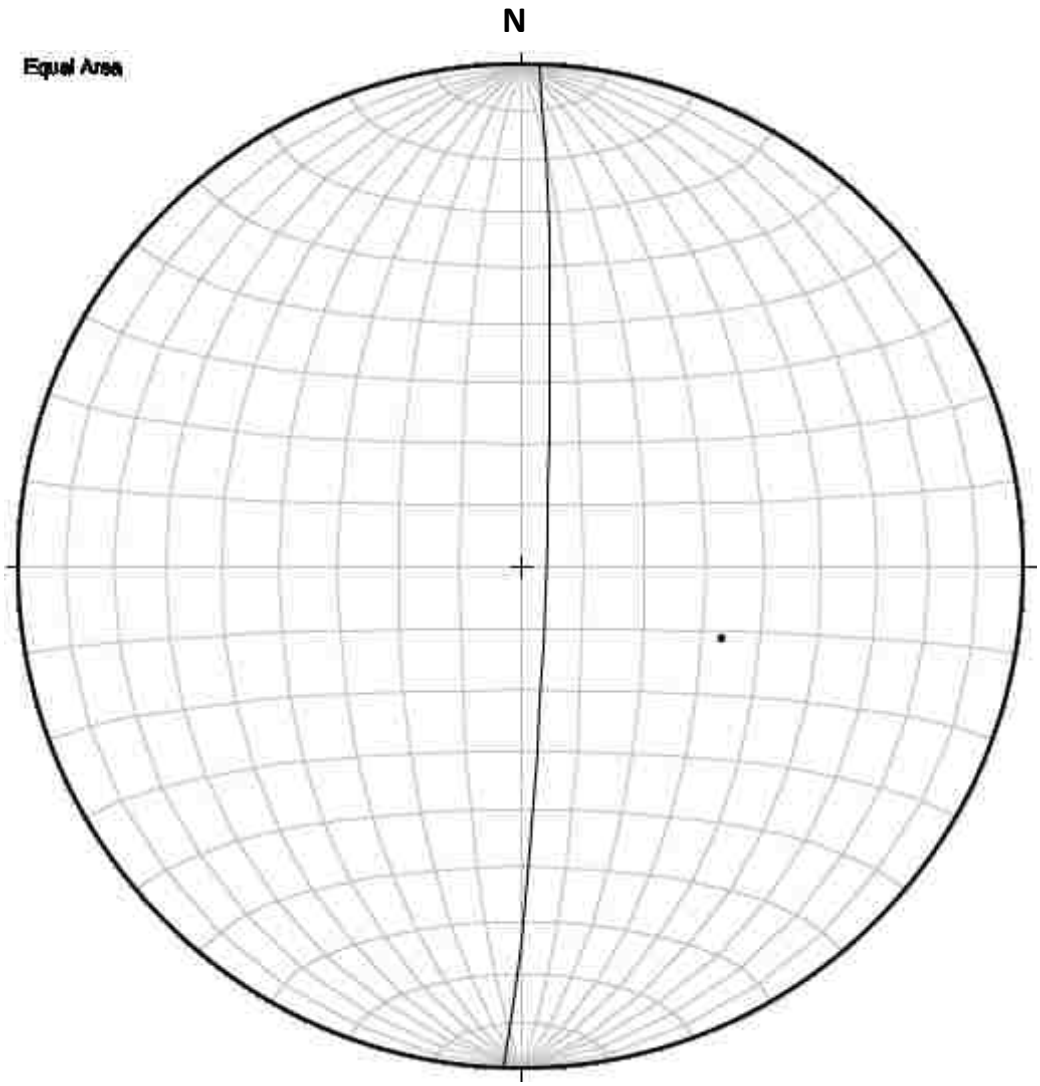

Figure 17. Stereograph with fault striking 2°, dipping 86° and slickenlines from fault set B.

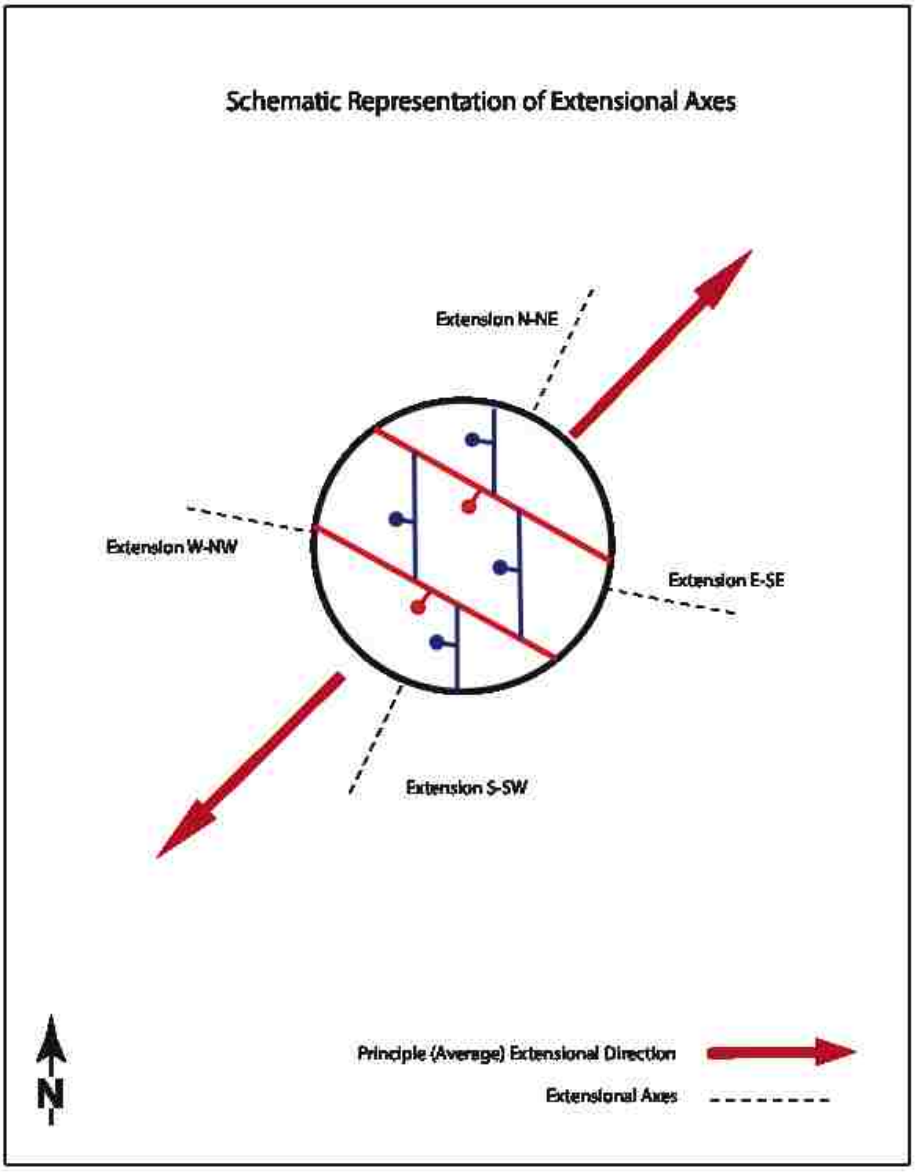

Figure 18. Schematic representation of primary extensional axis based on structural analysis. Dashed lines represent extensional axes determined from this study: NNE-SSW and WNW-ESE. Red arrows are the average of both NNE-SSW and WNW-ESE extensional axes and represent approximate extensional direction.

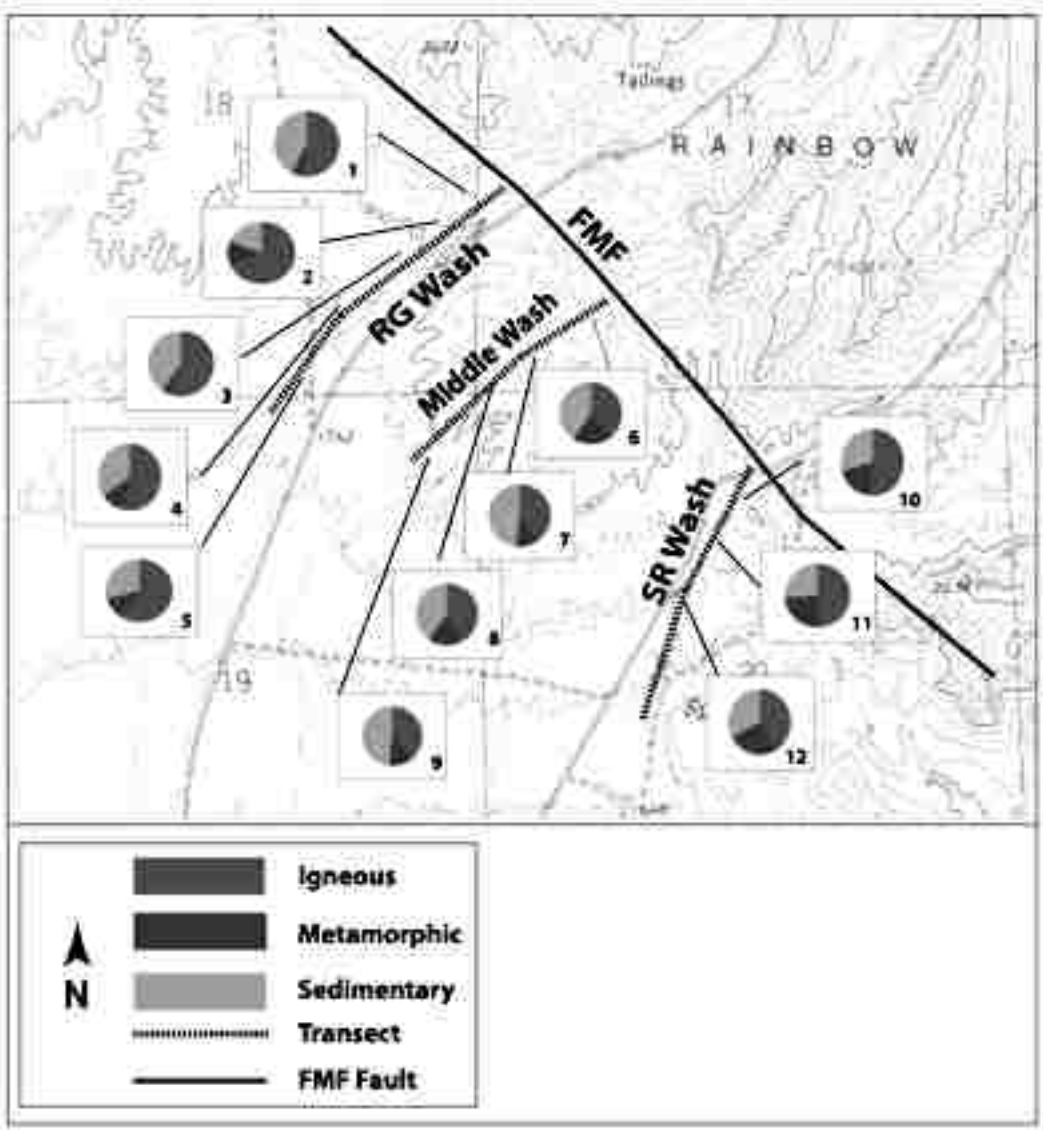

Figure 19. Topographic map of the field area in the northern section of the Henderson Quadrangle. Conglomerate clast counts were taken along three transects: RG = Rainbow Gardens wash, SR = southern road wash. Frenchman Mountain fault (FMF).

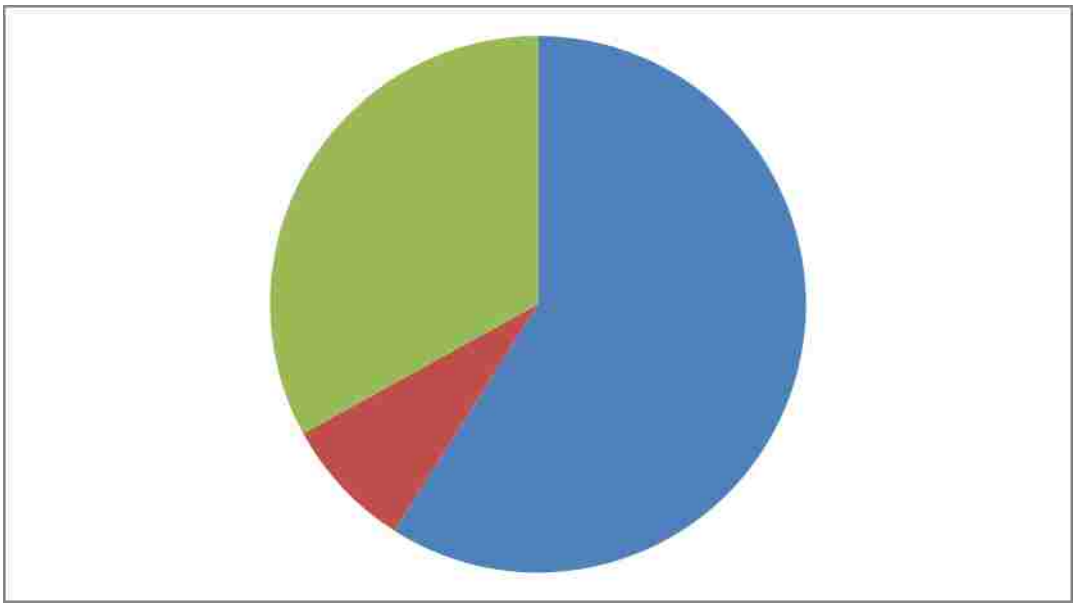

Figure 20. One pie chart showing provenance of conglomerate clasts from the Rainbow Gardens wash, representing the average of five clast counts taken along a transect within the Red Sandstone unit. Blue indicates igneous clasts (59 %), green indicates sedimentary clasts (33 %), and red indicates metamorphic clasts (8 %).

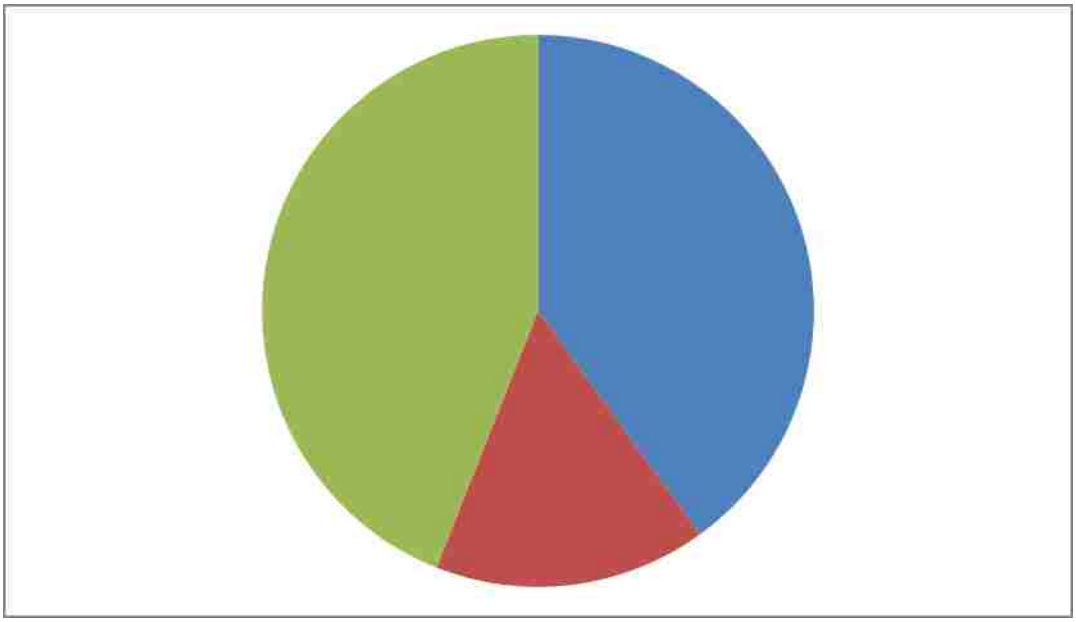

Figure 21. One pie chart showing provenance of conglomerate clasts from the middle wash, representing the average of four clast counts taken along a transect within the Red Sandstone unit. Blue indicates igneous clasts (40 %), green indicates sedimentary clasts (44 %) , and red indicates metamorphic clasts (16 %).

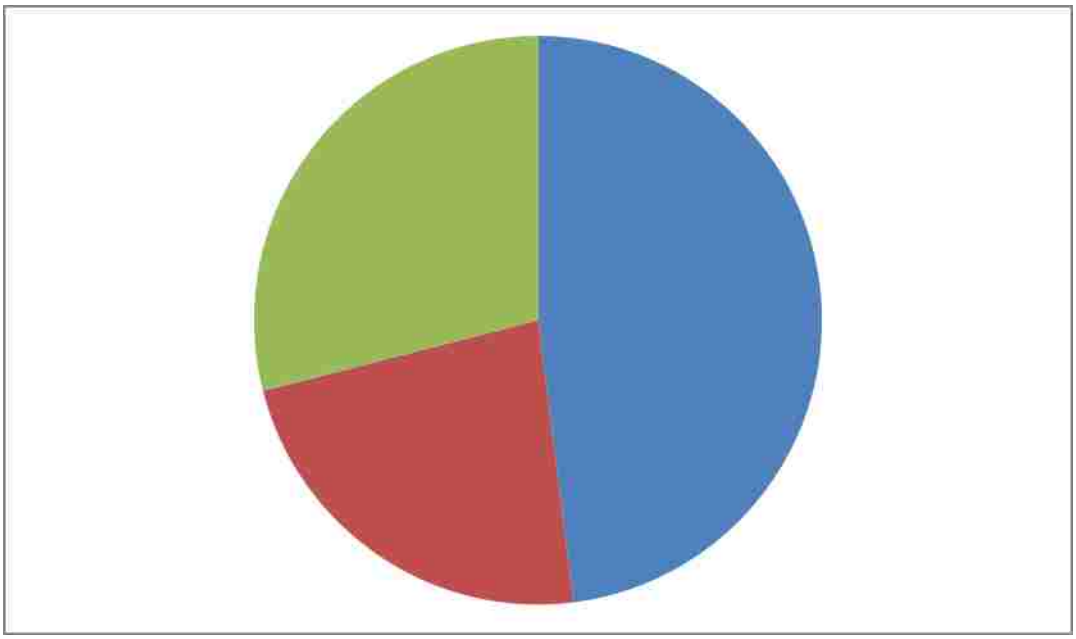

Figure 22. One pie chart showing provenance of conglomerate clasts from the southern road wash, representing the average of four clast counts taken along a transect within the Red Sandstone unit. Blue indicates igneous clasts (48 %), green indicates sedimentary clasts (29 %) , and red indicates metamorphic clasts (23 %).

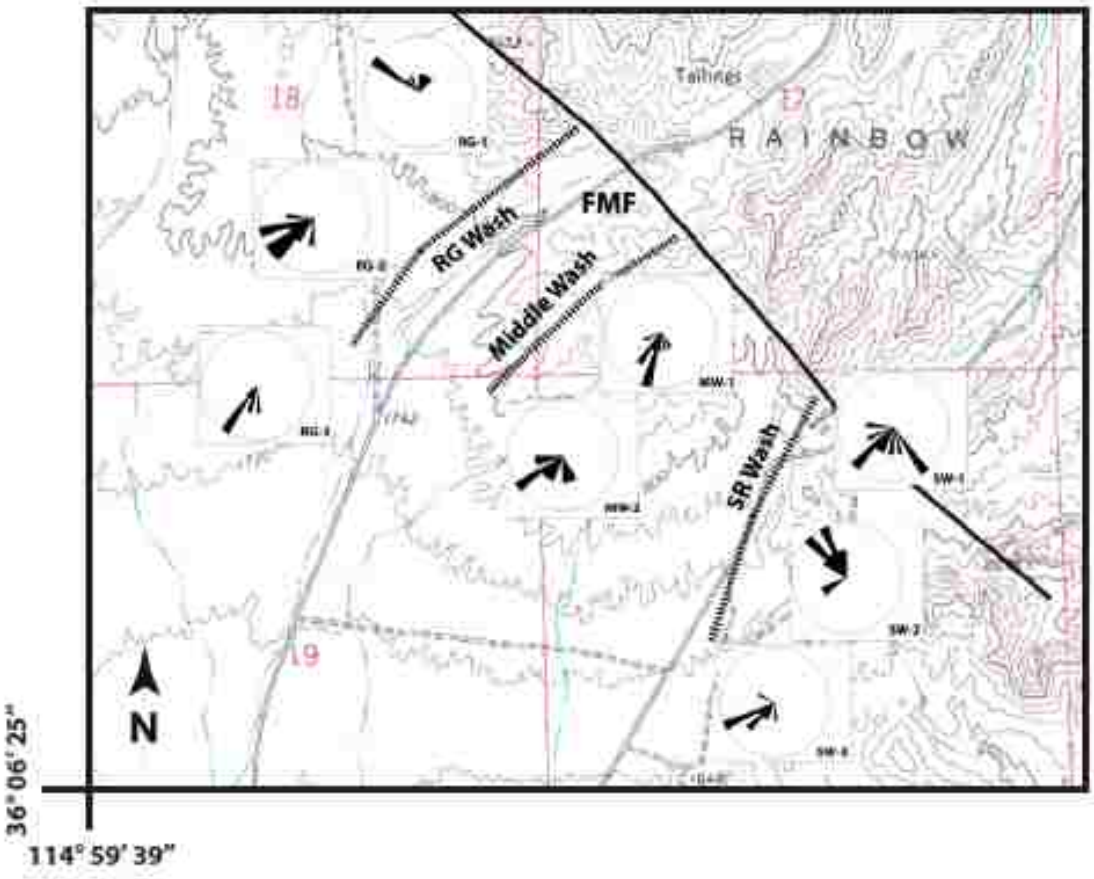

Figure 23. Topographic map of the field study area with locations of rose diagrams from paleocurrent taken within the Red Sandstone unit from imbricated clasts within interbedded conglomerate.

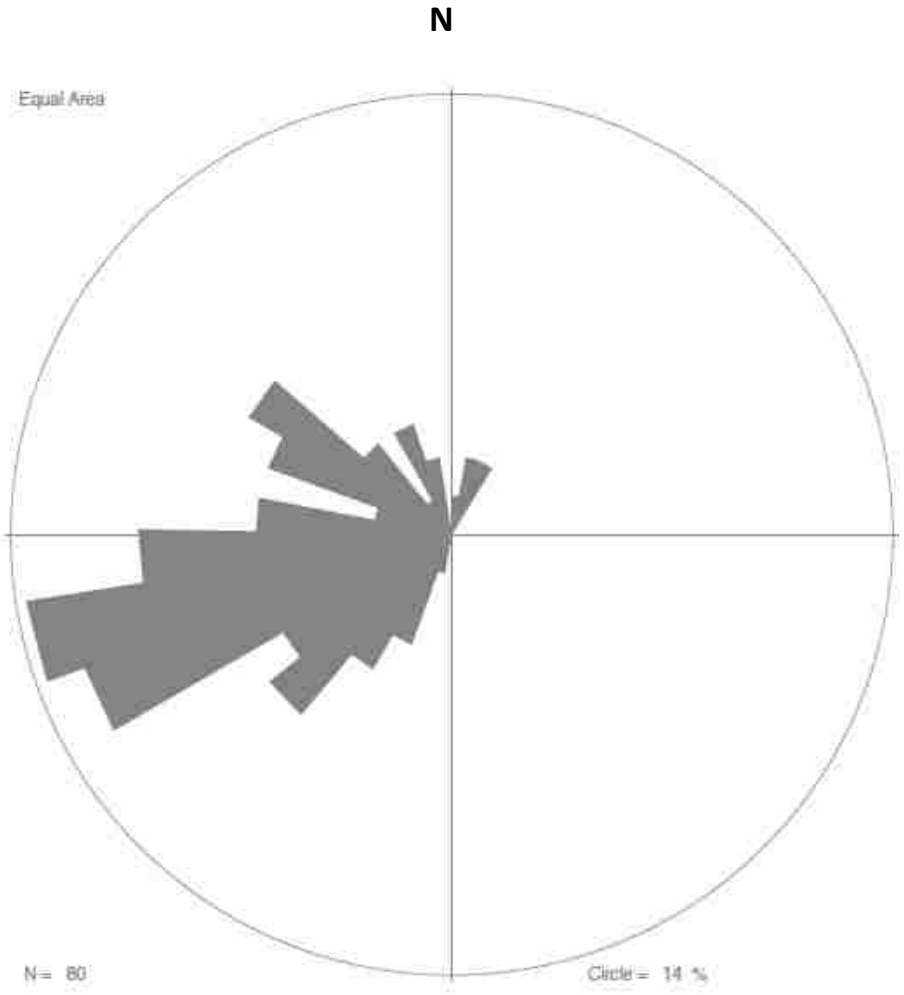

Figure 24. Paleocurrent diagram representing all paleocurrent data taken. Paleocurrent data were taken from imbricated clasts within interbedded conglomerate from within the basin fill of the field study area. All paleocurrent data were taken within the Red Sandstone unit.

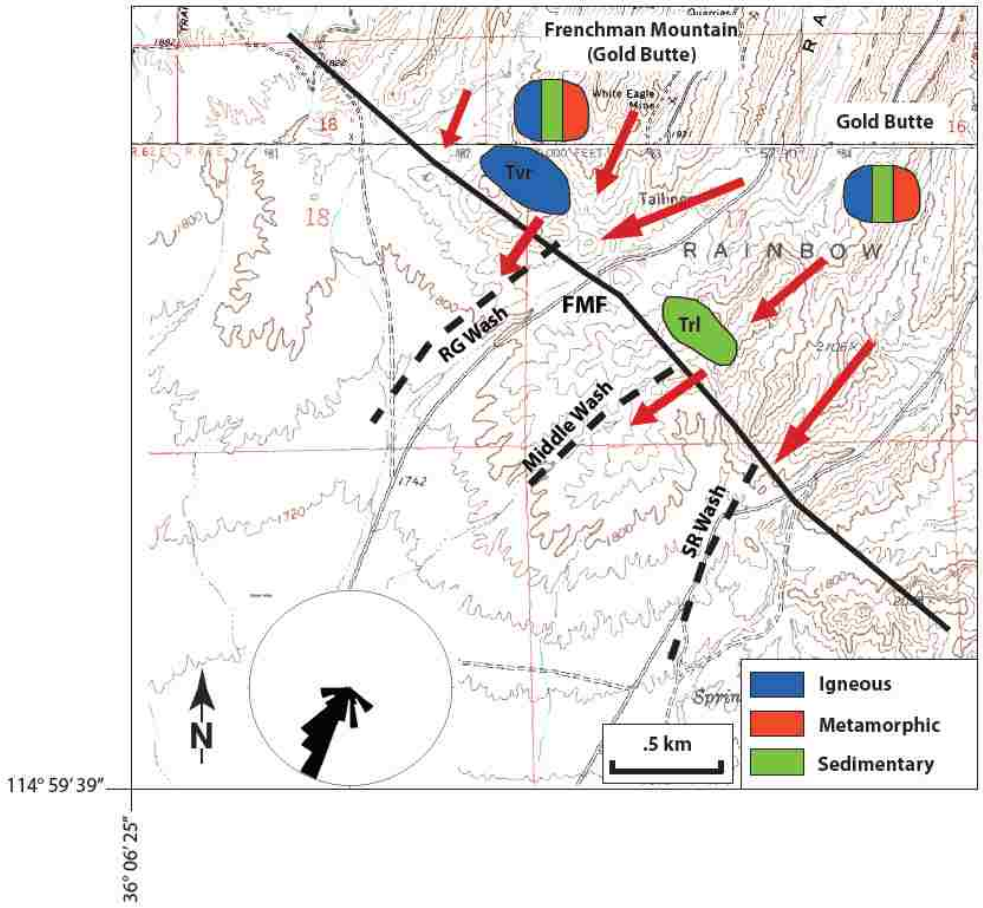

Figure 25. Schematic diagram showing hypothesized method of transport of detritus from the footwall onto the hanging wall, directly across the FMF with no lateral movement.

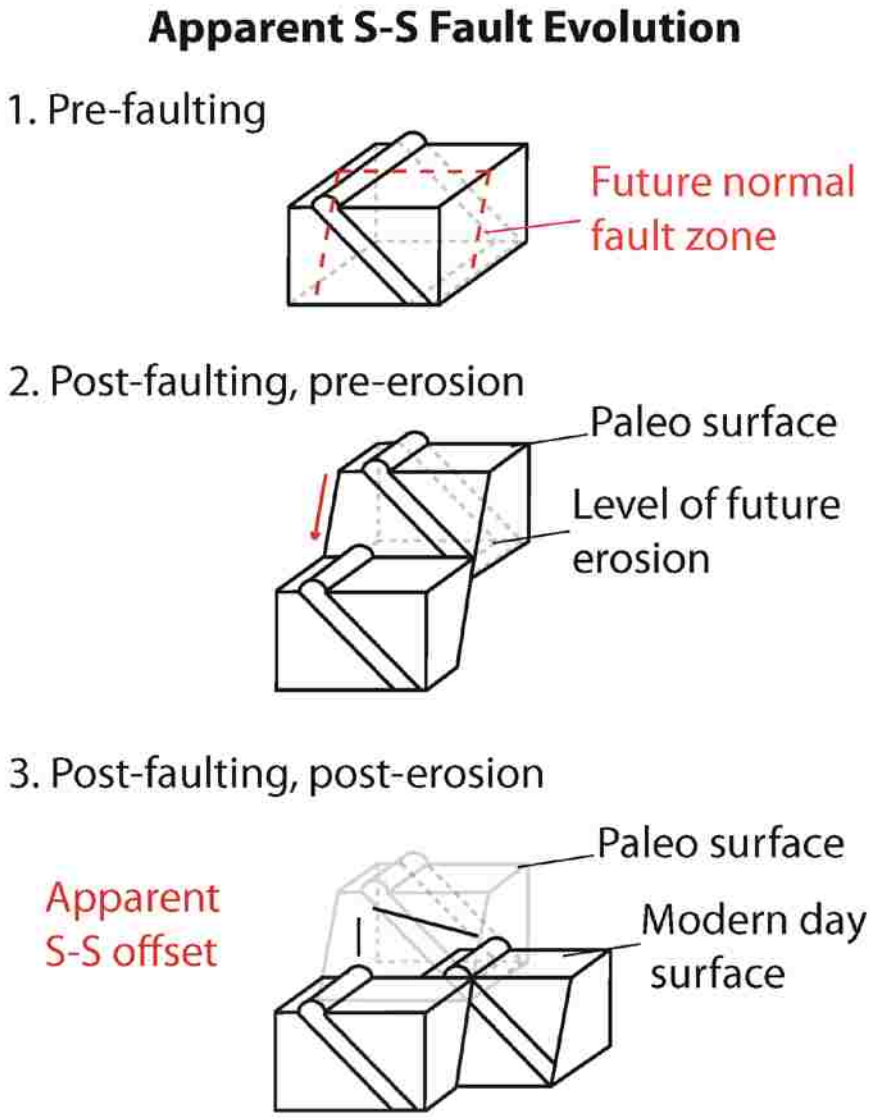

Figure 26. Schematic diagram showing the previously proposed apparent strike-slip offset as we interpret as normal faulting. 1) Pre-faulting geology, resistant marker bed is shown as a guide. 2) Post normal faulting, pre-erosive stage. Paleosurface and level of future erosion are shown. 3) Post-faulting, post-erosion, paleo surface and modern day surface are shown. Result is apparent strike-slip offset.

APPENDIX II

STRUCTURAL AND STRATIGRAPHIC DATA

Structural and kinematic data are listed in the tables below. All bedding orientations were taken using right hand rule: Pk = Kaibab limestone. Pkh = Harrisburg Member. Q = all Quaternary units. Tht = Thumb sandstone, siltstone, and conglomerate. Tr = Red Sandstone undifferentiated. Trr = Rainbow Gardens sandstone, conglomerate, and limestone. Trc = Rainbow Gardens resistant basal conglomerate. Trms = Moenkopi Schnabkaib Member. Trmu = Moenkopi Upper redbed unit. Trmv = Moenkopi Virgin Member. Trl = Rainbow Gardens reistant limestone unit. Ttb = Thumb Breccia with Proterozoic detritus. Ttc = Thumb Conglomerate. Ttg = Thumb Gypsum-rich sequence. Tvr = Volcanic Rocks of Rainbow Gardens nondifferentiated.

Table of bedding and fault data		
Type	Unit	Orientation
Bedding	Pk	24,43
Bedding	Pkh	58,29
Bedding	Pkh	30,33
Bedding	Pkh	67,38
Fault	Pkh/Trc	164,61
Bedding	Q	160,4
Bedding	Q	110,7
Bedding	Q	121,19
Bedding	Q	200,12
Bedding	Q	85,32
Bedding	Tht	124,35
Bedding	Tht	120, 26

Table of bedding and fault data		
Type	Unit	Orientation
Bedding	Tht	84,45
Bedding	Tht	98,82
Bedding	Tht/Tr	136,21
Bedding	Tht	93,64
Bedding	Tht	132,44
Bedding	Tht	93,68
Bedding	Tht	87,33
Bedding	Tht	103,72
Bedding	Tht	106,75
Bedding	Tht	101,67
Bedding	Tht	84,67
Bedding	Tht	132,43
Bedding	Tht	104,40
Bedding	Tht	100,74
Bedding	Tht	160,63
Bedding	Tht	125,40
Fault	Tht/Tht	110,45
Fault	Tht/Tr	155,65
Fault	Tht/Trr	134,76
Bedding	Tht/Trr	104,49
Bedding	Tht	104,32
Bedding	Tht	135,39
Bedding	Tht	131,24
Bedding	Tht	70,25
Bedding	Tht	48,32
Fold	Tht	30, 168

Table of bedding and fault data (Continue)		
Type	Unit	Orientation
Bedding	Tr	90,19
Bedding	Tr	136,39
Bedding	Tr	61,32
Bedding	Tr	68, 28
Bedding	Tr	35, 32
Bedding	Tr	27,35
Bedding	Tr/Q	29,6
Fault	Tr/Q	204,75
Fault	Tr/Tht	137,75
Bedding	Trc	60,42
Bedding	Trc	72,38
Bedding	Trc	48,35
Bedding	Trc	66,46
Bedding	Trc	53,20
Bedding	Trc	64,35
Fault	Trc/Trc	174,64
Fault	Trc/Trc	186,70
Fault	Trc/Trc	350,76
Fault	Trc/Trc	349, 79
Fault	Trc/Trc	179,67
Fault	Trc/Trr	162,80
Bedding	Trl	110,49
Bedding	Trl	114,43
Bedding	Trl	77,39
Bedding	Trms	52,24
Bedding	Trms	93,26

Table of bedding and fault data (Continued)		
Type	Unit	Orientation
Bedding	Trmu	50,53
Bedding	Trmu	96,24
Bedding	Trmu	40,29
Bedding	Trmv	56,38
Bedding	Trr	68,23
Bedding	Trr	98,22
Bedding	Trr	93,23
Bedding	Trr	119,70
Bedding	Trr	98,30
Bedding	Trr	105,35
Bedding	Trr	98,30
Bedding	Trr	96,50
Fault	Trr/Trc	165,70
Fault	Trr/Trl	188,74
Fault	Trr/Trmv	136,63
Bedding	Ttb	95,36
Bedding	Ttb	143,24
Fault	Ttb/Tr	320,65
Fault	Ttb/Tr	106,55
Bedding	Ttc	110,36
Bedding	Ttc	105,37
Bedding	Ttc	96,85
Bedding	Ttg	67,33
Bedding	Ttg	100,44
Bedding	Ttg	103,69
Fault	Ttg/Ttc	184,51

APPENDIX III

KINEMATIC DATA

Structural and kinematic data collected in the field. All bedding orientations were taken using right hand rule. Key for abbreviations can be found in Appendix I.

Table of kinematic data			
Type	Units	Measurements	Fault Set
Fault	Trr/Trmv	136,63	A
Fault	Tht/Trr	134,76	A
Fault	Tr/Tht	137,75	A
Fault	Tht/Tht	110,45	A
Fault	Ttb/Tr	106,55	A
Fault	Tvr	2,86	B
Fault	Trr/Trc	165,70	B
Fault	Trms/Trc	160,40	B
Fault	Trr/Trl	188,74	B
Fault	Pkh/Trc	164,61	B
Fault	Tr/Q	204,75	B
Fault	Trc/Trr	162,80	B
Fault	Trc/Trc	174,64	B
Fault	Trc/Trc	186,70	B
Fault	Trc/Trc	179,67	B
Fault	Ttg/Ttc	184,51	B
Fault	Tht/Tr	155,65	B
Fault	Trc/Trc	350,76	C
Fault	Trc/Trc	349, 79	C
Fault	Ttb/Tr	320,65	C

Table of paired fault and slicken measurement data		
Type	Units	Measurements
Fault	Tvr	2,86
Slickens		55 @ 110
Fault	Trc/Trr	162,80
Slickens		60 @ 176
		54 @ 230
		65 @ 229
		64 @ 253
		65 @ 253
		69 @ 231
		73 @ 250
		70 @ 246
Mullions		68 @ 80
		65 @ 76
		68 @ 80
Fault	Trc/Trc	186,70
Slickens		74 @ 257
		69 @ 266
Fault	Trc/Trc	350,76
Slickens		73 @ 110
		73 @ 112
		78 @ 168
Fault	Trc/Trc	179,67
Slickens		57 @ 243
		66 @ 290
		54 @ 241
		70 @ 233
		70 @ 234
		65 @ 223
Fault	Trc/Trc	349,79
Slickens		80 @ 45
		72 @ 53
		78 @ 43

Table of paired fault and slicken measurement data		
Type	Unit	Measurements
		77 @ 43
Fault	Ttg/Ttc	184,51
Slickens		33 @ 336
		36 @ 328
		25 @ 335

APPENDIX IV

CONGLOMERATE CLAST COUNT DATA

Conglomerate clast count data taken in the field study area. Location map showing clast counts is seen in Figure 19.

Table of conglomerate clast count data												
Clast Type	RG Wash	RG Wash	RG Wash	RG Wash	RG Wash	Middle Wash	Middle Wash	Middle Wash	Middle Wash	SR Wash	SR Wash	SR Wash
Clast Count Number	1	2	3	4	5	6	7	8	9	10	11	12
(I) Vesicular Basalt	14	3	6	4	6	0	2	2	0	2	4	3
(I) Volcanic (other basalt)	29	1	7	9	2	0		2	0	0	1	0
(I) Felsic plutonic (intermediate)	3	40	12	8	6	0	44	42	45	55	56	44
(I) Green plutonic	0	21	0	0	0	0	0	1	0	2	4	1
(I) Milky quartz	0	2	2	6	9	6	0	0	0	1	1	0
(I) Megacrystic Igneous (plagioclase)	6	0	37	19	26	35	0	0	0	0	0	0
(I) Amphibolite	0	2	0	0	0	0	0	0	0	0	0	0
(I) Subtotal	52	69	64	46	49	41	46	47	45	60	66	48
% (I)	52.5	69.7	56.1	55	60.5	39	40	42	38.7	51.2	48.8	42.1
(M) Gneiss	5	11	4	9	9	22	13	19	15	23	34	29
(M) Subtotal	5	11	4	9	9	22	13	19	15	23	34	29
% (M)	5.1	11.1	3.5	10.7	11.1	20.8	11.3	17	12.9	19.6	25.1	25.4
(S) Sandstone (red)	38	11	29	14	9	29	29	25	31	11	15	16
(S) Conglomerate	3	4	10	11	11	1	12	8	10	12	11	6

Table of conglomerate clast count data												
(S) Carbonate	1	3	7	4	3	13	14	11	15	11	9	15
(S) Siltstone	0	1	0	0	0	0	0	0	0	0	0	0
(S) Subtotal	42	19	46	29	23	43	55	44	56	34	35	37
% (S)	42.4	19.2	40.4	34.5	29.4	40.6	47.8	39.6	48.2	29	25.9	32.4
Unknown	0	0	0	0	1	1	1	1	0	0	0	0
Total	99	99	114	84	81	106	115	111	116	117	135	114
Clast Type												
% (I)	52.5	69.7	56.1	55	60.5	39	40	42	38.7	51.2	48.8	42.1
% (M)	5.1	11.1	3.5	10.7	11.1	20.8	11.3	17	12.9	19.6	25.1	25.4
% (S)	42.4	19.2	40.4	34.5	29.4	40.6	47.8	39.6	48.2	29	25.9	32.4

APPENDIX V

PALEOCURRENT DATA

Paleocurrent data, taken from a bed within the Red Sandstone Undifferentiated unit taken from imbricated clasts within interbedded conglomerate. Paleocurrent clast orientations were taken using the right hand rule, bedding orientations are included as well as the estimated paleoflow direction taken in the field.

Table of Paleocurrent data								
Name	SW-1	SW-2	SW-3	RG-1	RG-2	RG-3	MW-1	MW-2
Bedding Orientation	180, 36	25, 28	115, 30	95, 35	185, 35	172, 37	189, 36	220, 50
Estimated	SE	SE	SE	S	S	SE	S?	S
1	263, 45	309, 31	208, 37	335, 38	260, 41	225, 36	245, 47	300, 46
2	260, 46	311, 48	220, 49	340, 30	250, 43	252, 41	250, 38	303, 36
3	253, 41	300, 40	210, 54	349, 31	256, 32	218, 44	240, 64	298, 40
4	256, 48	314, 53	199, 52	5, 29	271, 50	240, 36	253, 50	292, 34
5	270, 53	309, 36	211, 50	334, 34	275, 35	230, 24	247, 43	295, 51
6	224, 38	265, 32	215, 40	20, 41	263, 28	240, 31	243, 35	286, 41
7	247, 40	260, 39	207, 41	338, 39	251, 32	241, 32	272, 46	288, 61
8	238, 55	305, 36	255, 45	20, 32	266, 30	240, 36	260, 51	298, 28
9	249, 59	310, 48	227, 29	10, 36	256, 54	225, 32	234, 49	279, 32
10	229, 62	324, 39	230, 35	10, 41	252, 39	205, 28	235, 55	290, 34

APPENDIX VI

PASSIVE SEISMIC DATA

Passive seismic low-frequency data is shown below. The lines were ran using 50 4.5 Hz 3-C geophones, with lines that were 2500 meters long with 50 meter spacing.

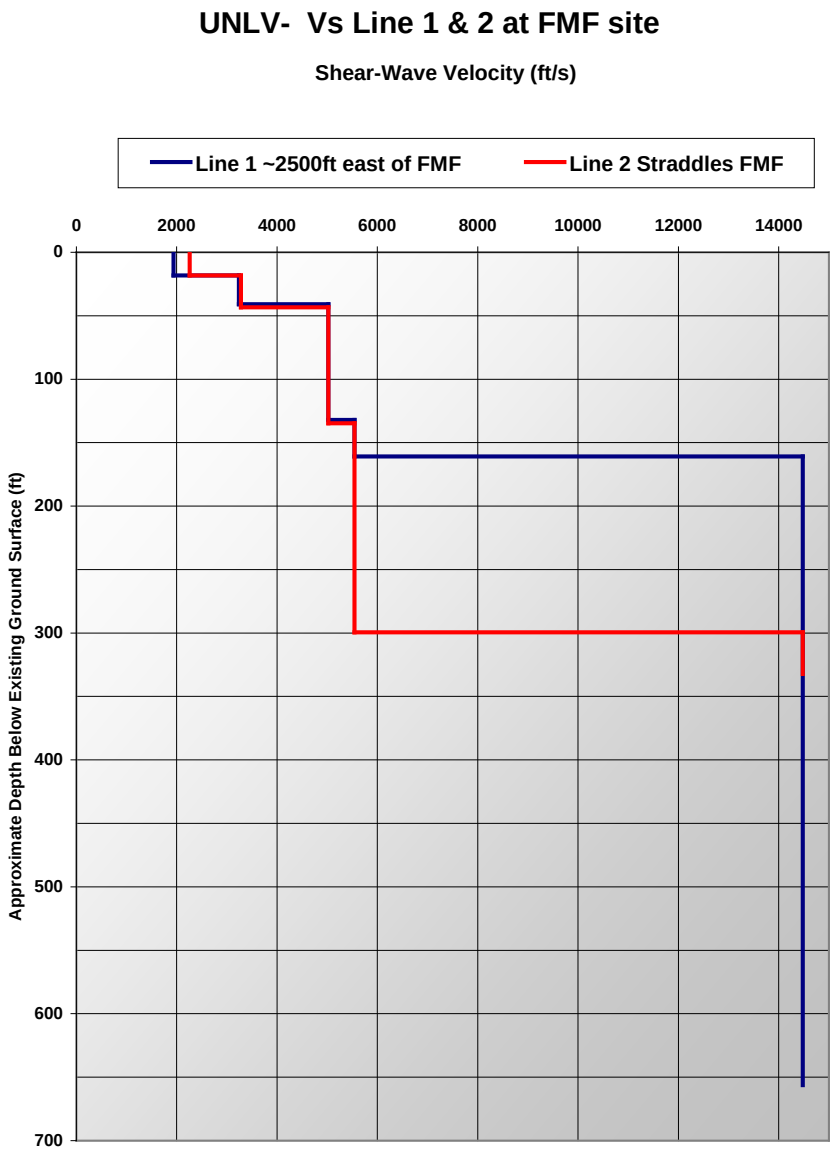

REFERENCES

Allmendinger, R.W., Stereonet Software, 2002: http://www.geo.cornell.edu/geology/faculty/RWA/programs.html2002.

Anderson, R.E., 1971, Large magnitude late Tertiary strike-slip faulting north of Lake Mead, Nevada: U.S. Geological Survey Professional Paper 794, 18.

Anderson, R.E., Barnhard, T.P., and Snee, L.W., 1994, Roles of plutonism, midcrustal flow, tectonic rafting, and horizontal collapse in shaping the Miocene strain field of the Lake Mead area, Nevada and Arizona: Tectonics, v. 13, p. 1381-1410.

Angelier, J., Colletta. B., and Anderson, R.E., 1985, Neogene paleostress changes in the Basin and Range: A case study at Hoover Dam, Nevada-Arizona: Geological Society of America Bulletin, v. 96, p. 347-361.

Beard, L.S., 1996, Paleogeography of the Horse Spring Formation in relation to the Lake Mead fault system, Virgin Mountains, Nevada and Arizona; Reconstructing the history of Basin and Range extension using sedimentology and stratigraphy: Special Paper - Geological Society of America, v. 303, p. 27-60.

Beard, L.S., Anderson, R.E., Block, D.L., Bohannon, R.G., Brady, R.J., Castor, S.B., Duebendorfer, E.M., Faulds, J.E., Felger, T.J., Howard, K.A., Kuntz, M.A., and Williams, V.S., 2007, Preliminary geologic map of the Lake Mead 30’ X 60’ quadrangle, Clark County, Nevada, and Mohave County, Arizona: United States Geological Survey, scale 1:100,000.

Bell, J.W., and Smith, E.I., 1980, Geologic map of the Henderson Quadrangle, Nevada: Nevada Bureau of Mine and Geology, Reno, NV, United States (USA), Report 67.

Bohannon, R.G., 1979, Strike-slip faults of the Lake Mead region of southern Nevada; Cenozoic paleogeography of the western United States: Pacific Coast Paleogeography Symposium, p. 129-139.

Bohannon, R.G., 1984, Nonmarine sedimentary rocks of Tertiary age in the Lake Mead region, southeastern Nevada and northwestern Arizona: U. S. Geological Survey, Reston, VA, United States (USA), Report P-1259, 72.

Bohannon, R.G., Grow, J.A., Miller, J.J., and Blank, R.H., Jr., 1993, Seismic stratigraphy and tectonic development of Virgin River depression and associated basins, southeastern Nevada and northwestern Arizona: Geologic Society of America Bulletin, v. 105, p. 501-520.

Burchfiel, B.C., Lipman, P.W., and Zoback, M.L.C., editors, 1992, The Cordilleran orogen, conterminous U.S. Boulder, Colo., Geological Society of America, v. G-3, p. 724.

Campagna, D.J., and Aydin, A., 1994, Basin genesis associated with strike-slip faulting in the Basin and Range, southeastern Nevada: Tectonics, v. 13, p. 327-341.

Castor, S.B., Faulds, J.E., Rowland, S.M., and dePolo, C.M., 2000, Geologic map of the Frenchman Mountain Quadrangle, Clark County, Nevada: Nevada Bureau of Mines and Geology, Reno, NV, United States (USA), Report 127, 25.

Dicke, S.M., 1990, Stratigraphy and sedimentology of the Muddy Creek Formation, southeastern Nevada [M.S. Thesis]: University of Kansas, 36.

Duebendorfer, E.M., Beard, L.S., and Smith, E.I., 1998, Restoration of Tertiary deformation in the Lake Mead region, southern Nevada; the role of strike-slip transfer faults; Accommodation zones and transfer zones; the regional segmentation of the Basin and Range Province: Special Paper - Geological Society of America, v. 323, p. 127-148.

Duebendorfer, E.M., and Simpson, D.A., 1994, Kinematics and timing of Tertiary extension in the western Lake Mead region, Nevada: Geological Society of America Bulletin, v. 106, p. 1057-1073.

Duebendorfer, E.M., and Wallin, E.T., 1991, Basin development and syntectonic sedimentation associated with kinematically coupled strike-slip and detachment faulting, southern Nevada: Geology, v. 19, p. 87-90.

Druschke, P., Hanson, A.D., Wells, M.L., 2008, Detrital zircon provenance of Cretaceous to Eocene strata in Sevier hinterland, central Nevada; implications for tectonics and paleogeography: Geological Society of America Abstracts with Programs, v. 40, no. 1, p. 78.

Druschke, P.A., Hanson, A.D., Wells, M.L., 2009, Structural, stratigraphic and geochronological evidence for extension predating Palaeogene volcanism in the Sevier hinterland, east-central Nevada: International Geology Review, v. 51, no. 7-8, p. 743-775.

Faulds, J.E., Feuerbach, D.L., Miller, C.F., and Smith, E.I., 2001, Cenozoic evolution of the northern Colorado River extensional corridor, southern Nevada and northwest Arizona: Utah Geologial Association Publication, v. 78, p. 239-272.

Forrester, S.W., 2009, Provenance of the Miocene-Pliocene Muddy Creek Formation Near Mequite, Nevada [M.S. thesis]: Las Vegas, University of Nevada, Las Vegas, 160.

Fyxell, J.E., and Duebendorfer, E.M., 1990, Origin and trajectory of the Frenchman Moutain block, southern Nevada: Geological Society of America Abstracts with Programs, v. 22, p. A226.

Fryxell, J.E., and Duebendorfer, E.M., 2005, Origin and trajectory of the Frenchman Mountain Block, an extensional allochthon in the Basin and Range Province, southern Nevada: Journal of Geology, v. 113, p. 355-371.

Guth, P.L., 1981, Tertiary extension north of the Las Vegas Valley shear zone, Sheep and Desert ranges, Clark County, Nevada: Geological Society of America Bulletin, v. 92, p. 763-771.

Hanson, A.D., Druschke, P.A., Howley, R.A., Surrmeyer, N.R., Benneman, B., Erwin, M.B., and McLaurin, B.T., 2005, Deformation of the Miocene-Pliocene Muddy Creek Formation, southern Nevada: Lake Mead Fault Systems, salt tectonics, or both? Geological Society of America Abstracts with Programs, v. 37, p. 42.

Heller, P.L., Bowdler, S.S., Chambers, H.P., Coogan, J.C., Hagen, E.S., Shuster, M.W., Winslow, N.S., and Lawton, T.W., 1986, Time of initial thrusting in the Sevier orogenic belt, Idaho, Wyoming, and Utah: Geology, v. 14, p. 388-391.

Humphreys, E., Hessler, E., Dueker, K., Farmer, G Lang, Erslev, E., and Atwater, T., 2003, How Laramide-age hydration of the North American lithosphere by the Farallon Slab controlled subsequent activity in the Western United States: International Geology Review, v. 45, no. 7, p. 575-595.

Lamb, M.A., Martin, L.K., Hickson, T.A., Umhoefer, P.J., and Eaton, L., 2010, Stratigraphy and age of the Lower Horse Spring Formation in the Longwell Ridges area, southern Nevada: Implications for tectonic interpretations: Geological Society of America Special Paper 463, p. 1-31.

Langenheim, V.E., Grow, J.A., Jachens, R.C., Dixon, G.L., and Miller, J.J., 2001, Geophysical constraints on the location and geometry of the Las Vegas Valley shear zone, Nevada: Tectonics, v. 20, p. 189-209

Longwell, C.R., 1974, Measure and Date of Movement on Las Vegas Valley Shear Zone, Clark County, Nevada: Geological Society of America Bulletin, v. 85, p. 985-989.

Longwell, C.R., 1971, Measure of lateral movement on Las Vegas shear zone, Nevada: Geological Society of America Abstracts with Programs, v. 3, p. 152.

Marrett, R., and Allmendinger R.W., 1990, Kinematic analysis of fault-slip data: Journal of Structural Geology, v. 12, p. 973-986.

Metcalf, L.A., 1982, Tephrostratigraphy and Potassium Argon determinations of seven volcanic ash layers in the Muddy Creek Formation of southern Nevada: Desert Research Institute and University of Nevada system publication 45023, 187.

Rittase, W.M., 2007, Cenozoic Extension in the River mountains and Frenchman mountain, southern Nevada [M.S. thesis]: Las Vegas, University of Nevada, Las Vegas, 160 p. 183.

Ron, H., Aydin, A., and Nur, A., 1989, Strike-slip faulting and block rotation in the Lake Mead fault system; response [modified]: Geology, v. 17, p. 1058.

Rowland, S.M., Parolini, J.R., Eschner, E., McAllister, A.J., and Rice, J.A., 1990, Sedimentologic and stratigraphic constraints on the Neogene translation and rotation of the Frenchman Mountain structural block, Clark County, Nevada; Basin and Range extensional tectonics near the latitude of Las Vegas, Nevada: Memoir - Geological Society of America, v. 176, p. 99-122.

Saenger, E.H., Schmalholz, S.M., Lambert, M.A., Nguyen, T.T., Torrest, A., Metzger, S., Habiger, R.M., Muller, T., Rentsch, S., Mendez-Hernandez, E., 2009, A passive

seismic survey over a gas field: Analysis of low-frequency anomalies: Geophysics, v. 74, p. 29-40.

Schweickert, R.A., Bogen, N.L., Girty, G.H., Hanson, R.E., and Merguerian C., 1984, Timing and structural expression of the Nevada orogeny, Sierra Nevada: Geological Society of America Bulletin, v. 95, p. 967-979.

Scott, A.J., 1988, The Muddy Creek Formation: Depositional environment, provenance, and tectonic significance in the western Lake Mead area, Nevada and Arizona [M.S. Thesis]: University of Nevada, Las Vegas, 114.

Sonder, L.J., and Jones, C.H., 1999, Western United States extension; how the west was widened: Annual Review of Earth and Planetary Sciences, v. 27, p. 417-462.

Taylor, W.J., and Switzer, D.D., 2001, Temporal changes in fault strike (to 90°) and extension directions during multiple episodes of extension: An example from eastern Nevada: Geological Society of America Bulletin, v. 113, p. 743-759

Trexler, J., and Cashman, P., 1991, Mississippian through Permian orogenesis in eastern Nevada: Post-Antler, pre-Sonoma tectonics of the western cordillera: American Association of Petroleum Geologists Conference, v. 75, p. 384.

Weber, M.E., and Smith, E.I., 1987, Structural and geochemical constraints on the reassembly of disrupted mid-Miocene volcanoes in the Lake Mead-Eldorado Valley area of southern Nevada: Geology, v. 15, p. 553-556.

Wernicke, B.P., Axen, G.J., and Snow, J.K., 1988, Basin and Range extensional tectonics at the latitude of Las Vegas, Nevada: Geological Society of America Bulletin, v. 100, p. 1738-1757

Wernicke, B., Spencer, J.E., Burchfiel, B.C., and Guth, P.L., 1982, Magnitude of crustal extension in the southern Great Basin: Geology (Boulder), v. 10, p. 499-503.

Williams, V.S., 1996, Preliminary geologic map of the Mesquite quadrangle, Clark and Lincoln Counties, Nevada and Mohave County, Arizona: U.S. Geological Survey Open-File Report 96-676.

VITA

Graduate College
University of Nevada, Las Vegas

Laura Margaret Eaton

Degrees:

Bachelor of Science, Geology, 2007
University of St. Thomas

Awards:

2009	Nevada Petroleum Society Research Grant
2009	UNLV Geoscience Department Scholarship
2009	UNLV Graduate College Scholarship
2007	University of St. Thomas Jack M. Brownstein Endowed Scholarship
2006	University of St. Thomas NASA Young Scholars Award

Publications:

Eaton, Laura M., Miley, William M., Lamb, Melissa, and Hickson, Thomas, T150. Understanding Mountain Belts from Basin-fill: Multi-disciplinary Approaches to the Detrital Record of Orogenic Evolution (Posters): Miocene Extensional Tectonics as Recorded by the Horse Spring Formation, Lake Mead Area, Nevada: Geochemical Ash Correlation within the Thumb Member. Geological Society of America Annual Convention, Technical Session: Poster Presentation. Philadelphia, PA. 2006.

Lamb, M.A., Martin, L., Hickson, T.A., Umhoefer, P.J., Eaton, L.M., Stratigraphy and age of the Lower Horse Spring Formation in the Longwell Riges area, southern Nevada: Implications for tectonic interpretations, in Umhoefer, P.J., Beard, L.S., and Lamb M.A., eds., Miocene Tectonics of the Lake Mead Region, Central Basin and Range: Geological Society of America Special Paper 463, pp. 1-31.

Thesis Title: Determining the Significance and Sense of Offset of the Frenchman Mountain Fault Near Las Vegas, Nevada: A Paired Basin Analysis and Structural Analysis

Thesis Examination Committee:

Chairperson, Dr. Andrew Hanson
Committee Member, Dr. Wanda Taylor
Committee Member, Dr. Eugene Smith
Graduate Faculty Representative, Dr. Susan Meacham